electrons in a magnetic field," *Phys. Rev. Letters*, vol. 2, pp. 504–505, June 15, 1959; "Negative elektrische leitfähigkeiten," *Z. Naturforsch*, vol. 15a, pp. 484–489, 1960.
[6] R. Q. Twiss, "Radiation transfer and the possibility of negative absorption in radio astronomy," *Austral. J. Phys.*, vol. 11, pp. 564–579, December 1958; also G. Bekefi, J. L. Hirshfield, and S. C. Brown, "Cyclotron emission from plasmas with non-Maxwellian distributions," *Phys. Rev.*, vol. 122, pp. 1037–1042, May 15, 1961.
[7] K. K. Chow, and R. H. Pantell, "A small-signal analysis of the electron cyclotron backward-wave oscillator," *IRE Trans. on Electron Devices*, vol. ED-9, pp. 351–358, July 1962.
[8] R. B. Hall, "Relativistic motion and energy gain of charged particles in a standing wave near cyclotron resonance," Boeing Scientific Research Labs., Seattle, Wash., Tech. Rept. D1-82-0388, 1964, unpublished.
[9] R. Le Gardeur, private communication.
[10] J. Feinstein, "Research on electron interactions with the fields of mirror resonators," *1964 Proc. Internat'l Congress on Microwave Tubes*, Paper 3F1.
[11] B. Lax and J. G. Mavroides, "Cyclotron resonance," in *Solid State Physics*, vol. 11. New York: Academic, 1960, pp. 261–388.
[12] P. A. Wolf, "Proposal for a cyclotron resonance maser in InSb," *Physics*, vol. 1, no. 3, pp. 147–158, 1964.
[13] I. B. Bernstein, "Waves in a plasma in a magnetic field," *Phys. Rev.*, vol. 109, pp. 10–21, January 1, 1958.
[14] H. Dreicer, "Enhanced radiation from ionized gases," *1963 Proc. VI Internat'l Conf. on Ionization Phenomena in Gases*, P. Hubert, ed. (S. E. R. M. A., Paris 1964), pp. 261–267.
[15] J. D. Coccoli, "Theory of fast-wave amplification of microwaves and electrons," Research Lab. of Electronics, M. I. T., Cambridge, Mass., Quart. Prog. Rept. 67, October 15, 1962, unpublished.
[16] P. Mallozzi and H. Margenau, "Absorption coefficient and microwave conductivity of plasmas," *Astrophys. J.*, vol. 137, pp. 851–857, April 1, 1963.
[17] G. Bekefi, J. L. Hirshfield, and S. C. Brown, "Kirchoff's radiation law for plasmas with non-Maxwellian distributions," *Phys. of Fluids*, vol. 4, pp. 173–176, February 1961.
[18] R. Wingerson, "'Corkscrew'—a device for changing the magnetic moment of charged particles in a magnetic field," *Phys. Rev. Letters*, vol. 6, pp. 446–448, May 1, 1961.
[19] D. C. Kelly, "The kinetic theory of a relativistic gas," 1963, unpublished.
[20] L. Mower and S. J. Buchsbaum, "Interaction between cold plasmas and guided electromagnetic waves II," *Phys. of Fluids*, vol. 5, pp. 1545–1551, December 1962.
[21] E. G. Harris, "Plasma instabilities associated with anisotropic velocity distributions," *J. Nucl. Energy*, vol. C2, pp. 138–145, January 1961.
[22] E. Weibel, "Spontaneously growing transverse waves in a plasma due to an anisotropic velocity distribution," *Phys. Rev. Letters*, vol. 2, pp. 83–84, February 1, 1959.
[23] J. L. Hirshfield, "Electron cyclotron maser: saturation," *1964 Proc. V Internat'l Congress on Microwave Tubes*, paper 3E1.
[24] W. E. Drummond and D. Pines, "Nonlinear plasma oscillations," *Annals of Physics*, vol. 28, pp. 478–499, July 1964.
[25] T. W. Hsu and P. N. Robson, "Negative absorption from weakly relativistic electrons traversing a Cuccia coupler," *Electronics Letters*, vol. 1, pp. 84–85, June 1965.

Theory of FM Laser Oscillation

S. E. HARRIS, MEMBER, IEEE, AND O. P. McDUFF, SENIOR MEMBER, IEEE

Abstract—**The paper presents a detailed analysis of FM laser oscillation which includes the effect of arbitrary atomic lineshape, saturation, and mode pulling. Such oscillation is achieved by means of an intracavity phase perturbation, and is a parametric oscillation wherein the laser modes oscillate with FM phases and nearly Bessel function amplitudes. One principal idea is that of the competition between different FM oscillations. The effect of the intracavity phase perturbation is to associate a set of sidebands with each of the previously free-running laser modes. While the free-running laser modes experienced their gain from essentially independent atomic populations, the competing FM oscillations to a large extent see the same atomic population; and in cases of interest the strongest of these oscillations is able to quench the competing weaker oscillations and establish the desired steady state condition. Results of the analysis include the following: threshold and power output, amplitudes and phases of all sidebands, frequency pulling of the entire oscillation, time domain behavior, distortion, supermode conversion efficiency, and effect of mirror motion. Results of numerical application of the theory to a number of specific cases are given.**

Manuscript received July 27, 1965; revised August 13, 1965. The work reported in this paper was supported by the Aeronautical Systems Division of the United States Air Force under Contract AF 33(657)-11144. O. P. McDuff was supported by a National Science Foundation Science Faculty Fellowship.

The authors are with the Department of Electrical Engineering, Stanford University, Stanford, Calif.

I. Introduction

THE ATOMIC populations which support most optical maser oscillation are, in general, sufficiently inhomogeneously broadened to allow oscillation in a large number of relatively independent axial modes. To a large extent, the gain of these modes results from their independent interaction with essentially different atomic populations. In gas masers, this is primarily the result of Doppler broadening [1], while in solid state masers it is often the result of what may be termed a spatial broadening [2] wherein, due to their differing spatial variation, the different optical modes interact with different atoms. Modes of the optical resonator which are located sufficiently close to the center of the atomic fluorescence line such that their single pass gain is greater than their single pass loss will oscillate. These modes are driven by spontaneous emission; they saturate nearly independently; and in most instances are, to a good approximation, uncoupled. The output of such multimode masers is not nearly as coherent as is desired for many of the applications of communication and spectroscopy.

In this paper we present a theoretical description of FM laser oscillation. Such oscillation was first demonstrated by Harris and Targ [3], and is a parametric oscillation wherein the atomic population is made to support a single coherent FM oscillation. FM laser oscillation is depicted schematically in Fig. 1, and is achieved by means of an element which allows the path length of the optical resonator to be rapidly varied. Such an element, which we term an intracavity phase perturbation, is driven at a frequency which is approximately, but not exactly, the frequency of the axial mode interval. The resulting laser oscillation consists of a set of modes which have nearly Bessel function amplitudes and FM phases, and which is, in effect, swept over a major portion of the fluorescence line at a sweep frequency which is that of the drive frequency of the phase perturbation.

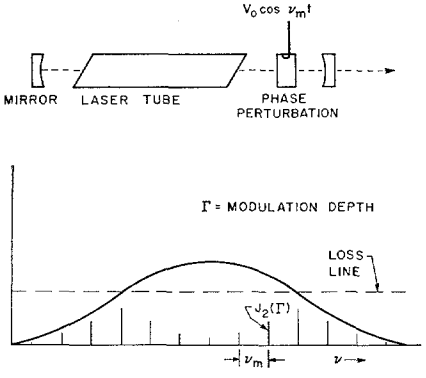

Fig. 1. Schematic of FM laser oscillation.

It will be seen that in order to achieve FM laser oscillation it is necessary for the intracavity phase perturbation to have a strength such that the parametric gain experienced by the laser modes is large compared with their net saturated atomic gains. From a physical point of view, the effect of the intracavity phase perturbation is to associate a set of FM sidebands with each of the previously free-running laser modes, i.e., to cause each of the previously free-running laser modes to become the center frequency or carrier of an FM signal. The resulting multiple FM oscillations then compete for the atomic population in the same sense as did the previously free-running modes. However, while the free-running modes experience their gain from essentially independent atomic populations, the competing FM oscillations, to a large extent, see the same atomic population. For instance, the first upper sideband of an FM oscillation which is centered in the atomic fluorescence line is in the same homogeneous linewidth and therefore sees the same atomic population as does the center frequency of an FM oscillation which is centered one mode above the center of the atomic fluorescence line. The competing FM oscillations are thus much more tightly coupled than were the previous free-running laser modes. In the cases of principal interest, the strongest of the FM oscillations—usually the oscillation whose carrier is at the center of the atomic line—will be able to completely quench the competing weaker oscillations. The result is that shown in the lower part of Fig. 1, wherein the sidesbands of a single coherent oscillation deplete most of the inverted population of the atomic line.

Many of the concepts applicable to free-running laser oscillation may be extended to apply to FM laser oscillation. The threshold of oscillation for a free-running laser mode occurs when gain exceeds loss. For FM laser oscillation, the gain and loss of a particular mode lose their significance, and we consider instead the threshold of the entire oscillation. This threshold will depend on the modulation depth of the oscillation and on a combination of the gains seen by all the FM sidebands. Similarly, instead of considering the pulling of a single free laser mode, we will consider the pulling of the entire FM oscillation.

The paper is divided into two major parts. Sections II through VIII develop the more analytical aspects of the theory, while Sections IX through XII give the results of numerical application of the theory to a number of specific cases and problems.

II. Development of the Basic Equations

We start with a set of equations derived by Lamb [4], termed as self-consistency equations, which describe the effect of an arbitrary optical polarization on the optical electric fields of a high-Q multimode optical resonator. They are as follows:

$$(\nu_n + \dot{\varphi}_n - \Omega_n)E_n = -\frac{1}{2}\left(\frac{\nu}{\epsilon_0}\right)C_n \tag{1a}$$

and

$$\dot{E}_n + \frac{1}{2}\left(\frac{\nu}{Q_n}\right)E_n = -\frac{1}{2}\left(\frac{\nu}{\epsilon_0}\right)S_n. \tag{1b}$$

In the foregoing equations, $E_n(t)$, ν_n, and $\varphi_n(t)$ are the amplitude, frequency, and phase, respectively, of the nth mode; and $C_n(t)$ and $S_n(t)$ are the in-phase and quadrature components of its driving polarization. That is, the total cavity electromagnetic field is given by

$$E(z, t) = \sum_n E_n(t) \cos [\nu_n t + \varphi_n(t)]U_n(z), \tag{2}$$

where $U_n(z) = \sin (n_0 + n)\pi z/L$.[1] The polarization driving the nth mode is obtained from

$$\begin{aligned} P_n(t) &= \frac{2}{L}\int_0^L P(z, t)U_n(z)\, dz \\ &= C_n(t) \cos [\nu_n t + \varphi_n(t)] + S_n(t) \sin [\nu_n t + \varphi_n(t)], \end{aligned} \tag{3}$$

where $P(z, t)$ is the total cavity polarization, and L is the cavity length. The addition of the integer n_0 to the cavity eigenfunction $U_n(z)$ is a departure from the notation of Lamb [4] but will lead to notational simplification in the following work. The integer n_0 is the number of spatial variations of some central mode, which

[1] Except where noted, all sums will be from $-\infty$ to $+\infty$.

we choose to be that mode whose frequency is closest to the center of the atomic fluorescence line. The circular frequency of this central mode is then $\Omega_0 = (n_0\pi c)/L$. Other symbols are defined as follows: $\Omega_n = \Omega_0 + (n\pi c)/L =$ frequency of the nth cavity resonance; $\Delta\Omega =$ frequency interval between axial resonances ($\Delta\Omega = \pi c/L$); $Q_n = Q$ of the nth mode; $\nu =$ average optical frequency.[2]

The total cavity polarization $P(z, t)$ consists of a parametric contribution resulting from the intracavity time varying phase perturbation, and of an atomic contribution resulting from the presence of the inverted atomic media. We assume the phase perturbation to have a time varying susceptibility $\Delta\chi'(z, t)$ of the form

$$\Delta\chi'(z, t) = \Delta\chi'(z) \cos \nu_m t, \tag{4}$$

where ν_m is the driving frequency of the perturbation. The parametric contribution to the total polarization $P(z, t)$ is then

$$\begin{aligned} P(z, t) &= \epsilon_0 \Delta\chi'(z, t) E(z, t) \\ &= \epsilon_0 \Delta\chi'(z) \cos \nu_m t E(z, t). \end{aligned} \tag{5}$$

Substituting (5) and (2) into (3), we find the component of $P(z, t)$ which drives the nth mode to be

$$P_n(t)_{\text{parametric}} = \frac{2\epsilon_0 \cos \nu_m t}{L} \sum_q E_q(t) \cos [\nu_q t + \varphi_q(t)] \cdot \int_0^L \Delta\chi'(z) U_q(z) U_n(z)\, dz. \tag{6}$$

We assume that the driving frequency ν_m is approximately equal to $\Delta\Omega$, and that the cavity Q's are sufficiently high that only the contributions of immediately adjacent modes need be retained. We thus keep only those terms of (6) for which $q = n \pm 1$. We define

$$\delta = \frac{\nu}{c} \int_0^L \Delta\chi'(z) U_{n\pm1}(z) U_n(z)\, dz, \tag{7}$$

which is the coupling coefficient between adjacent modes. The spatial variation of $\Delta\chi'(z)$ will generally be very slow compared with that of the cavity eigenfunction $U_n(z)$; thus by expanding (7) it is seen that δ is given by

$$\delta = \frac{1}{2} \frac{\nu}{c} \int_0^L \Delta\chi'(z) \cos \frac{\pi z}{L}\, dz. \tag{8}$$

Combining (6) and (7), we then have

$$P_n(t)_{\text{parametric}} = \frac{\epsilon_0 \delta c}{\nu L} \{E_{n+1}(t) \cos [(\nu_{n+1} - \nu_m)t + \varphi_{n+1}(t)] + E_{n-1}(t) \cos [(\nu_{n-1} + \nu_m)t + \varphi_{n-1}(t)]\}. \tag{9}$$

We may arbitrarily choose the frequency of the nth cavity mode ν_n to be any frequency in the vicinity of Ω_n. In that ν_n appears together with the unknown $\dot{\varphi}_n$, any error in its initial choice will be corrected in the solution by the appearance of a constant $\dot{\varphi}_n$. We let

$$\nu_n = \Omega_0 + n\nu_m,$$

and therefore

$$\begin{aligned} \nu_{n+1} - \nu_m &= \Omega_0 + (n+1)\nu_m - \nu_m = \nu_n \\ \nu_{n-1} + \nu_m &= \Omega_0 + (n-1)\nu_m + \nu_m = \nu_n. \end{aligned} \tag{10}$$

We introduce the atomic contribution to the polarization by means of macroscopic quadrature and in-phase components of susceptibility, denoted by χ_n'' and χ_n', respectively. Here χ_n'' and χ_n' depend upon E_n and therefore include the effects of atomic saturation, power dependent mode pulling and pushing, and nonlinear coupling effects. We resolve $P_n(t)$ of (9) into in-phase and quadrature components of the form of (3). Adding the atomic polarizability terms, $C_n(t)$ and $S_n(t)$ then becomes

$$C_n(t) = \epsilon_0 \chi_n' E_n + \frac{\epsilon_0 \delta c}{L} [E_{n+1} \cos (\varphi_{n+1} - \varphi_n) + E_{n-1} \cos (\varphi_n - \varphi_{n-1})] \tag{11a}$$

$$S_n(t) = \epsilon_0 \chi_n'' E_n + \frac{\epsilon_0 \delta c}{L} [-E_{n+1} \sin (\varphi_{n+1} - \varphi_n) + E_{n-1} \sin (\varphi_n - \varphi_{n-1})]. \tag{11b}$$

We define the detuning $\Delta\nu$ to be the frequency difference between the axial mode interval and the driving frequency of the internal phase perturbation, i.e., $\Delta\nu = \Delta\Omega - \nu_m$. We then have

$$\Omega_n - \nu_n = n\Delta\nu, \tag{12}$$

where positive $\Delta\nu$ denotes a driving frequency less than the axial mode interval. Substituting (11) and (12) into (1a) and (1b), we obtain

$$[\dot{\varphi}_n - n\Delta\nu + \tfrac{1}{2}\nu\chi_n']E_n = -\frac{\delta c}{2L} [E_{n+1} \cos (\varphi_{n+1} - \varphi_n) + E_{n-1} \cos (\varphi_n - \varphi_{n-1})] \tag{13a}$$

$$\dot{E}_n + \frac{\nu}{2}\left[\frac{1}{Q_n} + \chi_n''\right]E_n = \frac{\delta c}{2L} [E_{n+1} \sin (\varphi_{n+1} - \varphi_n) - E_{n-1} \sin (\varphi_n - \varphi_{n-1})], \tag{13b}$$

which are the fundamental equations of this paper and which, when solved, yield the amplitude, frequency, and phase of the optical modes. Equations (13a) and (13b) are to some extent equivalent to equations that have been given earlier by Gordon and Rigden [5], and by Yariv [6]. Except for notational changes, they are also equivalent to (5a) and (5b) of an earlier paper by Harris and McDuff [7].

III. Discussion of Parameters

For small signal conditions, the quadrature component of the atomic susceptibility χ_n'' is related to the single pass power gain by the relation

$$\frac{\nu L}{c} \chi_n'' = -g_n(1 - \sum_m \beta_{nm} E_m^2), \tag{14}$$

[2] We adopt the convention that all symbols for frequencies shall denote circular frequencies.

where g_n is the unsaturated single pass power gain of the nth mode, and the β_{nm} are saturation parameters which represent the effect of the mth mode on the gain of the nth mode [4].[3] Similarly, the in-phase component of the susceptibility may be expressed as

$$\frac{\nu L \chi_n'}{c} = \sigma_n + \sum_m \tau_{nm} E_m^2, \tag{15}$$

where σ_n is the additional round trip phase retardation which is seen by the nth mode as a result of power independent mode pulling, and the τ_{nm} represent power dependent pulling and pushing effects [4].

The Q of the nth mode may be written

$$\frac{\nu L}{c}\frac{1}{Q_n} = \alpha_n, \tag{16}$$

where α_n is the single pass power loss which is experienced by the nth mode as a result of nonzero output coupling, scattering, diffraction, etc. We note that Q_n is not meant to contain a contribution resulting from a parametric gain or loss; such contributions are accounted for by the right-hand side of (13b).

In practice, the time varying phase perturbation will often be achieved by means of a small perturbing element which has no significant spatial variation in the z direction, i.e., such that $\Delta\chi'(z)$ may be taken as independent of z over the length of the perturbing element. If we let δ_m denote the peak single pass phase retardation of such an element of length a, then it may readily be shown that

$$\delta_m = \frac{\Delta\chi' a \nu}{2c}. \tag{17}$$

If such an element is centered a distance z_0 from an end mirror of an optical cavity which has a total length L, then the coupling coefficient δ, as given by (8), becomes

$$\delta = \frac{\delta_m}{a}\int_{z_0-a/2}^{z_0+a/2} \cos\frac{\pi z}{L}\,dz, \tag{18}$$

which then yields

$$\delta = \frac{L}{a}\frac{2}{\pi}\left(\sin\frac{a}{L}\frac{\pi}{2}\right)\left(\cos\frac{z_0\pi}{L}\right)\delta_m. \tag{19}$$

If the length of the perturbing element is very small compared with the total length of the optical cavity ($a/L \ll 1$), then $\delta \cong \delta_m \cos(\pi z_0)/L$. It is, therefore, desirable for such a perturbing element to be situated as closely as possible to the end of the optical cavity. The coupling coefficient δ will then be very nearly the readily measurable peak single pass phase retardation of the perturbing element. It should be noted that if the perturbing element is not small, then its spatial variation may be of importance. As an extreme case, if the perturbing element were spatially uniform and completely filled the optical cavity, then δ would be zero.

[3] In writing (14) and (15), we have neglected terms which are dependent on the relative phases of the various optical modes. We also note that the notation of this section is not meant to correspond to that of Lamb [4].

IV. Steady State Solution of the Linear Approximation

In the present section we will neglect nonlinearities and take χ_n'' of all modes to be independent of E_n and equal to $-1/Q_n$. That is, we assume an infinity of laser modes, all having a single pass gain equal to their single pass loss. We also assume χ_n' to be zero, and look for solutions with $\dot{E}_n = 0$ and $\dot{\varphi}_n$ constant and independent of n. Equations (13a) and (13b) then become

$$[\dot{\varphi} - n\Delta\nu]E_n = -\frac{\delta c}{2L}[E_{n+1}\cos(\varphi_{n+1} - \varphi_n) + E_{n-1}\cos(\varphi_n - \varphi_{n-1})] \tag{20a}$$

$$0 = \frac{\delta c}{2L}[E_{n+1}\sin(\varphi_{n+1} - \varphi_n) - E_{n-1}\sin(\varphi_n - \varphi_{n-1})]. \tag{20b}$$

Noting the Bessel function identity

$$\frac{2n}{\Gamma}J_n(\Gamma) = J_{n+1}(\Gamma) + J_{n-1}(\Gamma), \tag{21}$$

we see that (20) is satisfied by the set of solutions

$$\begin{aligned} \dot{\varphi}_n &= q\Delta\nu \\ \varphi_{n+1} - \varphi_n &= 0 \\ E_n &= J_{n-q}(\Gamma), \end{aligned} \tag{22}$$

where q is an integer, and Γ is given by

$$\Gamma = \frac{c}{L}\frac{1}{\Delta\nu}\delta = \frac{1}{\pi}\frac{\Delta\Omega}{\Delta\nu}\delta = \frac{1}{\pi}\frac{\text{axial mode interval}}{\text{detuning frequency}}\delta. \tag{23}$$

We first consider the $q = 0$ solution, previously given by Harris and McDuff [7], and by Yariv [6], which is a perfect FM oscillation with a modulation depth of Γ and with a center frequency at the zeroth mode. From a varying frequency point of view, the peak-to-peak frequency swing of the oscillation is $2\Gamma\nu_m$. The modulation depth Γ is proportional to the strength of the time varying perturbation and inversely proportional to the detuning frequency $\Delta\nu$. The frequency of the nth cavity mode was originally defined as $\nu_n = \Omega_0 + n\nu_m$. Thus $n = 0$ denotes the only mode of the $q = 0$ solution whose oscillation frequency would, in the absence of the parametric phase perturbation, be a cavity resonance. A schematic of the $q = 0$ solution is shown in the upper part of Fig. 2. Consider next those solutions with $q \neq 0$. $\dot{\varphi} = q\Delta\nu$ denotes a uniform shift of all frequencies from their assumed positions by $q\Delta\nu$. For instance, if $q = 1$, all modes are shifted upward by $\Delta\nu$, and, as shown in the lower part of Fig. 2, the $n = 1$ mode is the only mode which is exactly on a cavity resonance. In this case the mode amplitudes are $E_n = J_{n-1}(\Gamma)$; and the $n = 1$ mode has amplitude $J_0(\Gamma)$ and is the center frequency of the FM oscillation. In a linear theory, any of the previously free-running laser modes may become the carrier of an FM oscillation. The carrier frequency of the qth oscillation is at the qth mode, and is distinguished in that its amplitude is $J_0(\Gamma)$ and in that it is the only sideband of that oscillation

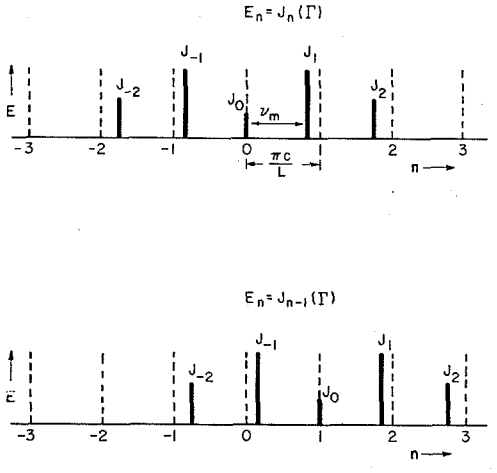

Fig. 2. Schematic of $q = 0$ and $q = 1$ solutions.

whose oscillation frequency is that of an original axial mode.

The total cavity electromagnetic field $E(z, t)$ which corresponds to a particular FM solution is obtained by substituting the solution of (22) into (2). Taking the case of $q = 0$, we have

$$E(z, t) = \sum_n J_n(\Gamma) \cos [(\Omega_0 + n\nu_m)t] \sin \frac{(n_0 + n)\pi z}{L}. \quad (24)$$

By the use of standard trigonometric and Bessel identities, $E(z, t)$ may be put into the closed form

$$E(z, t) = \tfrac{1}{2} \sin \left[\Omega_0 t + \frac{n_0 \pi z}{L} + \Gamma \sin \left(\nu_m t + \frac{\pi z}{L} \right) \right] - \tfrac{1}{2} \sin \left[\Omega_0 t - \frac{n_0 \pi z}{L} + \Gamma \sin \left(\nu_m t - \frac{\pi z}{L} \right) \right], \quad (25)$$

which corresponds to a forward and a backward FM traveling wave. We may further write this in standing wave form as

$$E(z, t) = \cos \left[\Omega_0 t + \Gamma \sin \nu_m t \cos \frac{\pi z}{L} \right] \cdot \sin \left[\frac{n_0 \pi z}{L} + \Gamma \cos \nu_m t \sin \frac{\pi z}{L} \right]. \quad (26)$$

It is of interest to note that the total cavity electromagnetic field at a particular point of space is in general not frequency modulated. In order to obtain a pure FM signal, it is necessary to couple to either, but not to both, of the FM traveling waves.

When $\Delta\nu = 0$, Γ, as defined by (23), is infinite, and the solutions considered thus far are indeterminant. In this case, (20a) and (20b) have the solution

$$\begin{aligned} E_n &= E_{n+1} \\ \varphi_{n+1} - \varphi_n &= p\pi \\ \dot{\varphi}_n &= (-1)^{p+1} \frac{\delta c}{L} = (-1)^{p+1} \frac{\delta}{\pi} \Delta\Omega, \end{aligned} \quad (27)$$

where p is an integer.

In the time domain, this solution corresponds to a behavior which consists of a repetitive series of pulses or spikes, with a pulsing frequency which is equal to the driving frequency of the internal phase perturbation. Such pulsing of a laser was first observed by Hargrove, Fork, and Pollack, and was obtained by acoustic modulation of the intracavity loss [8]. Linear analyses of intracavity loss modulation have been given by DiDomenico [9], Yariv [6] and Crowell [10].[4]

V. Dyadic Expansion of Steady State Equations

In the approximation of the previous section, nonlinearities and mode pulling were neglected, and an infinity of laser modes, all with gain equal to loss, were assumed. It was found that the sidebands comprising any of the FM oscillations had exactly Bessel function amplitudes and zero relative phases. That is, any FM oscillation was completely distortion free. When finite atomic linewidth, mode pulling, and atomic saturation are included, this is no longer the case. Relative amplitudes will no longer be exactly Bessel function, and the relative phases will no longer be exactly zero. In this and the following two sections, we develop an effective iterative procedure which will yield the amplitudes and phases of all sidebands of a particular oscillation, and also the center frequency, threshold, and power of the oscillation.

Implicit in the work of this section and of Section VII is the assumption that a stable, steady state solution of (13a) and (13b) exists. As will be seen in Section VIII, this will not always be the case. The general situation is that of a competition between different FM oscillations which are centered at different axial modes and which in the previous section were denoted by the integer q.

In particular, we will consider the $q = 0$ oscillation, i.e., that FM oscillation whose carrier frequency is closest to the center of the atomic line. In latter sections it will be seen that, in most cases of interest, it is this oscillation which will be dominant. Though the formulas will be given explicitly for the $q = 0$ oscillation, their extension to other oscillations will be apparent.

We seek a steady state solution to (13a) and (13b), and thus set $\dot{E}_n$ equal to zero and $\dot{\varphi}_n$ constant and independent of n. We define the quantities Ψ_n and ρ_n as follows:

$$\Psi_n = \frac{\nu L \chi_n'}{c} \quad (28a)$$

$$\rho_n = \frac{\nu L}{c} \left[\frac{1}{Q_n} + \chi_n'' \right]. \quad (28b)$$

Equations (13a) and (13b) may then be written

$$\left[\frac{2L}{\delta c} \dot{\varphi} - \frac{2n}{\Gamma} + \frac{\Psi_n}{\delta} \right] E_n = -[E_{n+1} \cos (\varphi_{n+1} - \varphi_n) + E_{n-1} \cos (\varphi_n - \varphi_{n-1})] \quad (29a)$$

[4] When $\Delta\nu = 0$, (20a) and (20b) also have solutions of the form $E_n = E_{n+1}$, $\varphi_{n+1} - \varphi_n = \pm\pi/2$, $\dot{\varphi}_n = 0$. However, during the course of the numerical analyses which will be described in later sections, solutions of this type were not observed.

$$\frac{\rho_n}{\delta} E_n = [E_{n+1} \sin(\varphi_{n+1} - \varphi_n) - E_{n-1} \sin(\varphi_n - \varphi_{n-1})], \tag{29b}$$

which are a set of simultaneous nonlinear difference equations. The quantity Ψ_n is the additional round trip phase retardation which is seen by the nth mode as a result of the real part of the atomic susceptibility and is described in (15). The quantity ρ_n, described in (14) and (16), is the net saturated single pass power gain of the nth mode. In a free-running laser, all modes oscillate at a power level such that single pass gain equals single pass loss, and therefore ρ_n is zero for all oscillating modes. In the presence of the parametric phase perturbation, this is no longer the case. For those modes which oscillate at a level which is greater than their free-running counterparts, ρ_n is positive; while for those modes which oscillate at a level which is less than their free-running counterparts, ρ_n is negative.

We first consider (29b). We treat the E_n and ρ_n as knowns, and solve for the relative phase angles $(\varphi_n - \varphi_{n-1})$. When considered in this way, (29b) is a linear, first-order, inhomogeneous difference equation with nonconstant coefficients (the E_n). We proceed by construction of a Green's dyadic $G_{n,q}$ such that

$$E_{n+1}G_{n+1,q} - E_{n-1}G_{n,q} = \delta_{n,q}, \tag{30}$$

where $\delta_{n,q}$ is the Kronecker delta [11]. The relative phase angles are then obtained from the relation

$$\sin(\varphi_n - \varphi_{n-1}) = \frac{1}{\delta} \sum_{q=-\infty}^{+\infty} G_{n,q}\rho_q E_q. \tag{31}$$

If we arbitrarily introduce the boundary condition that $G_{n,q} = 0$ at $n = -\infty$, we find the Green's dyadic satisfying (30), and this boundary condition is to be

$$\begin{aligned} G_{n,q} &= \frac{E_q}{E_n E_{n-1}} \qquad n > q \\ &= 0 \qquad\qquad n \leq q. \end{aligned} \tag{32}$$

The relative phase angles are then given by

$$\sin(\varphi_n - \varphi_{n-1}) = \frac{1}{E_n E_{n-1}} \frac{1}{\delta} \sum_{q=-\infty}^{n-1} \rho_q E_q^2. \tag{33}$$

Alternately, we could introduce the boundary condition $G_{n,q} = 0$ at $n = +\infty$. In this case the appropriate Green's dyadic is

$$\begin{aligned} G_{n,q} &= -\frac{E_q}{E_n E_{n-1}} \qquad n \leq q \\ &= 0 \qquad\qquad n > q, \end{aligned} \tag{34}$$

and the relative phase angles are obtained from

$$\sin(\varphi_n - \varphi_{n-1}) = -\frac{1}{E_n E_{n-1}} \frac{1}{\delta} \sum_{q=n}^{\infty} \rho_q E_q^2. \tag{35}$$

Though the relative phase angles which are predicted by (33) and (35) at first appear to be different, it will be seen that, due to a conservation condition to be proven in the following section, they are in fact identical.

We next consider the first of the steady state equations, i.e., (29a). We define a difference operator $\mathfrak{L}$ such that

$$\mathfrak{L}E_n = E_{n-1} - \frac{2n}{\Gamma} E_n + E_{n+1} \tag{36}$$

and a perturbation μ_n given by

$$\begin{aligned} \mu_n &= E_{n+1}[1 - \cos(\varphi_{n+1} - \varphi_n)] \\ &\quad + E_{n-1}[1 - \cos(\varphi_n - \varphi_{n-1})] - \left[\frac{\Psi_n}{\delta} + \frac{2L}{\delta c}\dot{\varphi}\right] E_n. \end{aligned} \tag{37}$$

In terms of these definitions, (29a) may be written

$$\mathfrak{L}E_n = \mu_n. \tag{38}$$

By means of the Bessel function identity of (21) and the orthogonality relation

$$\sum_{n=-\infty}^{+\infty} J_{n-q}(\Gamma)J_{n-p}(\Gamma) = \delta_{q,p}, \tag{39}$$

which is a form of Neumann's addition theorem for Bessel functions [12], it is seen that a complete and orthonormal set of eigenvectors $|u_q\rangle$, with corresponding eigenvalues λ_q of the operator $\mathfrak{L}$, are given by

$$\begin{aligned} |u_q\rangle &= J_{n-q}(\Gamma) \\ \lambda_q &= q\frac{2}{\Gamma}. \end{aligned} \tag{40}$$

Proceeding by spectral expansion [11], the operator which is inverse to $\mathfrak{L}$ may then be written

$$\mathfrak{L}^{-1} = \frac{\Gamma}{2} \sum_{\substack{q \\ q \neq 0}} \frac{1}{q} |u_q\rangle\langle u_q|. \tag{41}$$

The solution to (29a), or equivalently (38), is then given by

$$E_n = kJ_n(\Gamma) + \frac{\Gamma}{2} \sum_{\substack{q \\ q \neq 0}} \sum_m \frac{1}{q} J_{n-q}(\Gamma)J_{m-q}(\Gamma)\mu_m. \tag{42}$$

The first term on the right side of this equation is the homogeneous solution of (38), and has an amplitude constant k which is to be determined. The second term is a particular solution which results from the perturbation μ_n.

It is to be noted that (33) or, equivalently, (35), and (42) are all exact, and that no approximations have been made. These equations form the basis of the iterative procedure to be given in Section VII.

VI. Conservation Conditions

We next derive two conservation conditions which are also necessary for the iterative procedure. We return to (13b), multiply through by E_n, and sum both sides over n from $-\infty$ to $+\infty$. We then have

$$\begin{aligned} &\sum_n E_n\dot{E}_n + \frac{v}{2}\left[\frac{1}{Q_n} + \chi_n''\right]E_n^2 \\ &= \frac{\delta c}{2L} \sum_n [E_nE_{n+1} \sin(\varphi_{n+1} - \varphi_n) - E_nE_{n-1} \sin(\varphi_n - \varphi_{n-1})]. \end{aligned} \tag{43}$$

By the change of variable $n = n' + 1$, the second term on the right-hand side of this equation is equal to the first. We thus obtain

$$\sum_{n=-\infty}^{+\infty} E_n \dot{E}_n + \frac{\nu}{2}\left[\frac{1}{Q_n} + \chi_n''\right]E_n^2 = 0. \tag{44}$$

Noting that $E_n\dot{E}_n = (d/dt)(E_n^2/2)$, it is seen that the foregoing equation is a statement of power conservation. That is, the rate of change of total stored energy, plus the net power dissipated or absorbed in all modes, is zero. Though in the absence of the parametric phase perturbation power is conserved by all modes individually,[5] in its presence, power must be conserved jointly. It is noted that the phase perturbation itself does not contribute or absorb any power from the system.

In the steady state, all $\dot{E}_n = 0$, and (44) becomes

$$\sum_n \rho_n E_n^2 = 0, \tag{45}$$

where the ρ_n are the net saturated single pass power gains and are defined in (28b). Equation (45) establishes the equivalence of (33) and (35) of the previous section.

We apply a similar procedure to (13a). Multiplying through by E_n and summing over n from $-\infty$ to $+\infty$, we obtain

$$\sum_{n=-\infty}^{+\infty} [\dot{\varphi}_n - n\Delta\nu + \tfrac{1}{2}\nu\chi_n']E_n^2 = -\frac{\delta c}{L}\sum_{n=-\infty}^{+\infty} E_nE_{n+1}\cos(\varphi_{n+1} - \varphi_n), \tag{46}$$

which is a reactive conservation condition and which, when the relative steady state amplitudes and phases are known, will determine the frequency of oscillation.

VII Steady State Amplitudes, Phases, Frequency, and Power

As a result of nonzero net saturated gains, and due to the in-phase component of the atomic susceptibility χ_n', actual mode amplitudes and phases will not be exactly those of the ideal FM solution of Section IV. In this section we describe an iterative procedure which allows the calculation to any desired order of the relative mode amplitudes and phases, as well as the center frequency and power of an FM oscillation. The results of the first iteration will reveal the mechanism of the distortion and, are themselves useful for certain applications. The plan of the iterative procedure is to first assume the modes to have Bessel function relative amplitudes. By application of the power conservation condition of (45), the amplitude of the oscillation is determined. Net saturated gains are then obtained, and (33) or, equivalently, (35) is used to find the first-order relative phases. With relative phases known, the contribution to the amplitude perturbation μ_n [(37)], which is a result of the nonzero net saturated gains, may be found. The frequency pulling or pushing of the oscillation $\dot{\varphi}$ is then obtained from the reactive conservation condition of (46). With μ_n now determined, second-order amplitudes may be obtained from (42), and a second iteration may be begun.

In order to effectively illustrate this procedure, it is convenient to assume a specific form for the saturation of the atomic gain.[6] We choose completely inhomogeneous saturation, such that the single pass gain of the nth mode is given by $-g_n(1 - \beta E_n^2)$; i.e., in (14) we take $\beta_{nm} = \beta\delta_{nm}$ where β is a saturation parameter which is the same for all modes. The net saturated gain of the nth mode, as defined by (28b), then becomes

$$\rho_n = \alpha_n - g_n(1 - \beta E_n^2), \tag{47}$$

where α_n is the single pass power loss as given by (16). We let $E_n = kJ_n(\Gamma)$, and substitute from (47) into the power conservation condition of (45). We then have

$$\sum_n \{\alpha_n - g_n[1 - \beta k^2 J_n^2(\Gamma)]\}k^2 J_n^2(\Gamma) = 0. \tag{48}$$

Solving for the oscillation level k^2, we obtain

$$k^2 = \frac{1}{\beta}\frac{\sum_n (g_n - \alpha_n)J_n^2(\Gamma)}{\sum_n g_n J_n^4(\Gamma)}. \tag{49}$$

With the amplitude of all modes determined to first order, the net saturated gains are obtained from (47) with $E_n^2 = k^2 J_n^2(\Gamma)$. First-order relative phase angles are then obtained from (33) or (35). Using (33), we have

$$\sin(\varphi_n - \varphi_{n-1}) = \frac{1}{J_n(\Gamma)J_{n-1}(\Gamma)}\frac{1}{\delta}\sum_{q=-\infty}^{n-1}\rho_q J_q^2(\Gamma). \tag{50}$$

For the case of a symmetrical line shape wherein ρ_n is an even function of n, the evaluation of (50) is simplified by means of the relation

$$\sum_{q=-\infty}^{0}\rho_q J_q^2(\Gamma) = \tfrac{1}{2}\rho_0 J_0^2(\Gamma), \tag{51}$$

which is obtained from the conservation condition (45).

Two points concerning the relative phase angles may be noted. First, nonzero relative phase angles result from an accumulation of nonzero net saturated gains. In general, an FM laser operated at a Γ such that the relative mode amplitudes to at least some extent approximate those of a free-running laser will, at a given δ, have less phase distortion than will an FM laser whose mode amplitudes depart sharply from those of the free-running case. In particular, distortion will be increased when operating at a Γ such that the amplitude of some mode is driven close to zero; or alternately, when operating at a large Γ, such that a number of modes have amplitudes which are considerably larger than the corresponding free-running modes, for instance when Γ is such that the equivalent frequency swing is considerably larger than the spectral width of the free-running laser. In the first case, some particular ρ_n will become large

[5] This statement is strictly true only in the limit of completely inhomogeneous broadening.

[6] We note that this assumption is illustrative and not restrictive; and that the iterative procedure is valid, irrespective of the atomic lineshape and the type of saturation which is assumed.

and negative; in the second case, an accumulation of positive ρ_n's will result.

The second and very important point is that phase distortion may be made arbitrarily small by making the perturbation strength δ increasingly large. It is therefore desirable to obtain a given Γ by working with the largest available δ, and thus from (22) with a correspondingly large detuning.

With relative phases determined, we next find the first-order correction to the center frequency of the FM oscillation. We substitute $E_n = kJ_n(\Gamma)$ into the reactive conservation condition of (46), and note that in the steady state $\dot{\varphi}$ is constant and independent of n. Using the definition of Ψ_n of (28a), we then have

$$\dot{\varphi} = -\frac{c}{2L}\sum_n \Psi_n J_n^2(\Gamma) - \frac{c\delta}{L}\sum_n J_n(\Gamma)J_{n+1}(\Gamma)\cos(\varphi_{n+1} - \varphi_n), \quad (52)$$

where we have used the relation $\sum_{n=-\infty}^{+\infty} J_n^2(\Gamma) = 1$. The oscillation frequency of the nth axial mode is then $\Omega_0 + n\nu_m + \dot{\varphi}$, and the center frequency of the oscillation is thus $\Omega_0 + \dot{\varphi}$. Equation (52) describes to first order the frequency pulling or pushing of the entire FM oscillation. The first term on the right-hand side gives the contribution to the pushing or pulling which results from the presence of the atomic media, and is in fact simply the weighted average of the pushing or pulling which is associated with each of the laser modes. The second term is a parametric pushing or pulling term. By noting the Bessel identity $\sum_{n=-\infty}^{+\infty} J_n(\Gamma)J_{n+1}(\Gamma) = 0$, it is seen that for an ideal FM signal having relative phase angles which are all zero, the parametric term would be zero. This situation will be approached as δ becomes increasingly large. If Ω_0 is at the center of an exactly symmetrical atomic line, both the atomic and the parametric terms are zero, and the center frequency of the FM oscillation will be Ω_0.

The amplitude perturbation is now completely determined and given by

$$\mu_n = J_{n+1}(\Gamma)[1 - \cos(\varphi_{n+1} - \varphi_n)] + J_{n-1}(\Gamma)[1 - \cos(\varphi_n - \varphi_{n-1})] - J_n(\Gamma)\left[\frac{\Psi_n}{\delta} + \frac{2L}{\delta c}\dot{\varphi}\right]. \quad (53)$$

Substitution of μ_n into (42) yields a set of second-order amplitudes, and the first iteration is complete. The distortion which results from the nonzero net saturated gains is, to first order, phase distortion. At sufficiently large δ, the cosine of the relative phase angles approaches unity, and their contribution to μ_n nearly vanishes. The contribution to μ_n resulting from mode pulling also varies inversely as δ, and thus at large δ the μ_n approach zero; and from (40) the E_n approach $kJ_n(\Gamma)$.

As δ becomes increasingly large, (49) becomes an increasingly exact expression for the level of the FM oscillation. We note that the total power output of the FM oscillation is proportional to the total stored energy E_n^2, which for $E_n = kJ_n(\Gamma)$ equals k^2. From (49), we see that to first order the threshold for FM laser oscillation is given by

$$\sum_n (g_n - \alpha_n)J_n^2(\Gamma) > 0. \quad (54)$$

Equation (54) is the condition for positive power output in an FM laser, and is analogous to the condition $g_n > \alpha_n$ for threshold of a free-running laser. Typically, the cavity loss α_n will be the same for all modes, and (54) becomes

$$\sum_n g_n J_n^2(\Gamma) > \alpha, \quad (55)$$

where α is the single pass power loss of all modes. An FM laser will be above threshold if the sum of the weighted, unsaturated single pass gains is greater than the single pass loss. Note that in an FM laser this threshold condition depends on Γ, which in turn depends on both δ and on the detuning $\Delta\nu$. An FM laser may thus be extinguished by varying either δ or the driving frequency of the perturbation.

Application of the iterative procedure to particular cases, as well as discussion of its convergence, will be given later in the paper.

VIII. Competition and Quenching of FM Oscillations

In the previous section we examined the details of a single steady state FM oscillation, with the implicit assumption that such a stable steady state condition exists. The more general situation is that of a number of competing FM oscillations, with each previously free-running laser mode acting as the center frequency or carrier for a particular oscillation. While the free-running modes were very weakly coupled, the competing FM oscillations, to a large extent, see the same atomic population and are closely coupled. In many cases, the strongest of these oscillations is able to quench the weaker oscillations and thereby establish the desired steady state condition.

The purpose of this section is to develop a simplified set of equations which, to a good approximation, will describe the competition between the FM oscillations. The details of any particular oscillation will not be considered. That is, it will be assumed that δ is sufficiently large that the sidebands which comprise any of the FM oscillations have Bessel function amplitudes and FM phases.

The plan is to first show that a solution consisting of a sum of independent FM oscillations, each with arbitrary amplitude and arbitrary phase, satisfies (13a) and (13b) for an ideal system wherein gain equals loss for all modes. It will, in effect, be shown that the FM oscillations are the normal modes of the lossless system. The competition between oscillations will then be introduced by means of a statement of power conservation. The procedure could perhaps be considered analogous to that used in micro-

wave systems wherein the field configuration of the lossless system is used to take into account small losses.

In the multioscillation situation, each cavity mode contains sidebands from each of the FM oscillations. The variables E_n and φ_n are envelop quantities and become increasingly complicated as the number of FM oscillations is increased. It is, therefore, convenient to change to the new variables X_n and Y_n which are the in-phase and quadrature components, respectively, of a particular mode, as opposed to its amplitude and phase. We let

$$\begin{aligned} X_n &= E_n \cos \varphi_n \\ Y_n &= E_n \sin \varphi_n, \end{aligned} \tag{56}$$

and thus

$$\begin{aligned} E_n &= (X_n^2 + Y_n^2)^{1/2} \\ \tan \varphi_n &= \frac{Y_n}{X_n}. \end{aligned} \tag{57}$$

Taking appropriate partial derivatives of E_n and φ_n and substituting into (13a) and (13b), after some algebra we obtain the completely equivalent equations

$$X_n\dot{Y}_n - Y_n\dot{X}_n + (-n\Delta\nu + \tfrac{1}{2}\nu\chi_n')(X_n^2 + Y_n^2)$$

$$= -\frac{\delta c}{2L}[X_n(X_{n+1} + X_{n-1}) + Y_n(Y_{n+1} + Y_{n-1})] \tag{58a}$$

and

$$X_n\dot{X}_n + Y_n\dot{Y}_n + \frac{\nu}{2}\left[\frac{1}{Q_n} + \chi_n''\right][X_n^2 + Y_n^2]$$

$$= \frac{\delta c}{2L}[X_n(Y_{n+1} + Y_{n-1}) - Y_n(X_{n+1} + X_{n-1})]. \tag{58b}$$

The expected multioscillation solution has mode amplitudes E_n and mode phases φ_n such that

$$E_n(t) \cos [\nu_n t + \varphi_n(t)]$$

$$= \sum_{q=-\infty}^{+\infty} a_q J_{n-q}(\Gamma) \cos [\nu_n t + q\Delta\nu t + \theta_q], \tag{59}$$

where a_q and θ_q are the amplitude and phase, respectively, of the component FM oscillations, and are assumed to be independent of time. As in Section IV, the integer q denotes that mode which is the center frequency of a particular FM oscillation. Expanding (59), we have

$$E_n \cos \varphi_n \cos \nu_n t - E_n \sin \varphi_n \sin \nu_n t$$

$$= \sum_q a_q J_{n-q}(\Gamma) \cos (q\Delta\nu t + \theta_q) \cos \nu_n t$$

$$- \sum_q a_q J_{n-q}(\Gamma) \sin (q\Delta\nu t + \theta_q) \sin \nu_n t. \tag{60}$$

By separately equating in-phase and quadrature components, we see that the expected solution is given by

$$\begin{aligned} X_n(t) &= \sum_q a_q J_{n-q}(\Gamma) \cos (q\Delta\nu t + \theta_q) \\ Y_n(t) &= \sum_q a_q J_{n-q}(\Gamma) \sin (q\Delta\nu t + \theta_q). \end{aligned} \tag{61}$$

It may be shown that, for the ideal lossless case wherein $Q_n = -\chi_n''$ and $\chi_n' = 0$ for all n, the $X_n(t)$ and $Y_n(t)$ of (61) identically satisfy (58a) and (58b). This is true regardless of the amplitude a_q or the phase θ_q of the respective FM oscillations. If nonlinearities are neglected, an FM laser is no better than a free-running laser. As opposed to a set of uncoupled free-running modes, we find a set of uncoupled FM oscillations. These oscillations may be independently excited and might be considered as the normal modes of the lossless system. In the actual situation wherein net saturated gains and χ_n' are not zero, X_n and Y_n will not satisfy (58a) and (58b). That is, the sidebands which comprise each of the FM oscillations will not have exactly Bessel function amplitudes and zero relative phases. However, as δ is increased it is expected that the above solution should become increasingly exact.

We now make use of power conservation to introduce the effects of atomic saturation. To start, the total average stored energy $\mathcal{E}$ of all modes is given by

$$\begin{aligned} \mathcal{E} &= \tfrac{1}{2}\sum_n E_n^2(t) \\ &= \tfrac{1}{2}\sum_n X_n^2(t) + Y_n^2(t), \end{aligned} \tag{62}$$

which in terms of the a_q and θ_q of (61) becomes

$$\mathcal{E} = \tfrac{1}{2}\sum_n \sum_q \sum_p a_q a_p J_{n-q}(\Gamma) J_{n-p}(\Gamma)$$

$$\cdot \cos [(q - p)\,\Delta\nu t + (\theta_q - \theta_p)], \tag{63}$$

where we have used the trigonometric identity for the cosine of a difference of angles. We sum over n, and make use of the orthogonality condition of (39). We then have

$$\mathcal{E} = \tfrac{1}{2}\sum_q \sum_p a_q a_p \cos [(q - p)\,\Delta\nu t + (\theta_q - \theta_p)]\,\delta_{q,p} \tag{64}$$

and thus

$$\mathcal{E} = \tfrac{1}{2}\sum_q a_q^2. \tag{65}$$

We next calculate the total power $\mathcal{P}$ which is absorbed or dissipated by all modes. From the conservation condition (44), $\mathcal{P}$ is given by

$$\mathcal{P} = \frac{\nu}{2}\sum_n \left(\frac{1}{Q_n} + \chi_n''\right)E_n^2. \tag{66}$$

We assume small signal saturation of the form of (14). Using (16), we have

$$\mathcal{P} = \frac{c}{2L}[\sum_n (\alpha_n - g_n)E_n^2 + \sum_n \sum_m g_n\beta_{nm}E_m^2E_n^2]. \tag{67}$$

In terms of the X_n and Y_n, $\mathcal{P}$ is given by

$$\mathcal{P} = \frac{c}{2L}[\sum_n (\alpha_n - g_n)(X_n^2 + Y_n^2)$$

$$+ \sum_n \sum_m g_n\beta_{nm}(X_n^2X_m^2 + X_m^2Y_n^2 + X_n^2Y_m^2 + Y_m^2Y_n^2)]. \tag{68}$$

Consider first the term $X_n^2X_m^2$. For brevity, we let

$$\xi_q = q\Delta\nu t + \theta_q. \tag{69}$$

Substituting from (61), we have

$$X_n^2X_m^2 = \sum_q \sum_l \sum_s \sum_r a_q a_l a_s a_r J_{n-q}(\Gamma)J_{n-l}(\Gamma) \cdot J_{m-s}(\Gamma)J_{m-r}(\Gamma)\cdot\cos\xi_q\cdot\cos\xi_l\cdot\cos\xi_s\cdot\cos\xi_r. \quad (70)$$

The product of four cosines may be expanded to yield

$$\tfrac{1}{8}[\cos(\xi_q+\xi_l-\xi_s-\xi_r)+\cos(\xi_q-\xi_l+\xi_s-\xi_r)+\cos(\xi_q-\xi_l-\xi_s+\xi_r)+\cos(\xi_q+\xi_l+\xi_s+\xi_r)+\cos(\xi_q+\xi_l+\xi_s-\xi_r)+\cos(\xi_q+\xi_l-\xi_s+\xi_r)+\cos(\xi_q-\xi_l+\xi_s+\xi_r)+\cos(\xi_q-\xi_l-\xi_s-\xi_r)].$$

In summing (70), we will keep only those terms which are independent of the ξ_i, and thereby neglect the effects of a possible phase locking of FM oscillations. Summing over r and s, we find that for $q \neq l$ the first of the above cosine terms contributes the phase independent term

$$\tfrac{1}{4}\sum_q \sum_{\substack{l \\ q\neq l}} a_q^2a_l^2J_{n-q}(\Gamma)J_{n-l}(\Gamma)J_{m-q}(\Gamma)J_{m-l}(\Gamma)$$

to the sum of (70), while for $q = l$, it contributes

$$\tfrac{1}{8}\sum_q a_q^4J_{n-q}^2(\Gamma)J_{m-q}^2(\Gamma).$$

Proceeding similarly, we find contributions from the second and third of the foregoing cosine terms. Examination of each of the last five of those cosine terms shows that, since their arguments do not contain an equal number of plus and minus signs, these terms do not contribute any terms which are independent of the ξ_i. Adding all contributions, we find the phase independent portion of $X_n^2X_m^2$ to be

$$X_n^2X_m^2 = \tfrac{1}{2}\sum_q\sum_l a_q^2a_l^2J_{n-q}(\Gamma)J_{n-l}(\Gamma)J_{m-q}(\Gamma)J_{m-l}(\Gamma) + \tfrac{1}{4}\sum_q\sum_l a_q^2a_l^2J_{n-q}^2(\Gamma)J_{m-l}^2(\Gamma) - \tfrac{3}{8}\sum_q a_q^4J_{n-q}^2(\Gamma)J_{m-q}^2(\Gamma). \quad (71a)$$

We next evaluate the contribution of the other terms of (68). Proceeding as before, we find their phase independent contribution to be

$$Y_m^2Y_n^2 = X_n^2X_m^2 \quad (71b)$$

and

$$X_m^2Y_n^2 = \tfrac{1}{4}\sum_q\sum_l a_q^2a_l^2J_{n-q}^2(\Gamma)J_{m-l}^2(\Gamma) - \tfrac{1}{8}\sum_q a_q^4J_{m-q}^2(\Gamma)J_{n-q}^2(\Gamma) \quad (71c)$$

$$X_n^2Y_m^2 = X_m^2Y_n^2 \quad (71d)$$

and

$$X_n^2 + Y_n^2 = \sum_q a_q^2J_{n-q}^2(\Gamma). \quad (71e)$$

Combining the contributions of (71a)–(71e), we find the total phase independent power which is dissipated or absorbed by all modes to be given by

$$\mathcal{P} = \frac{c}{2L}[\sum_n\sum_q(\alpha_n - g_n)a_q^2J_{n-q}^2(\Gamma) + \sum_n\sum_m\sum_q\sum_l g_n\beta_{nm}a_q^2a_l^2J_{n-q}(\Gamma)J_{n-l}(\Gamma)J_{m-q}(\Gamma)J_{m-l}(\Gamma) + \sum_n\sum_m\sum_q\sum_l g_n\beta_{nm}a_q^2a_l^2J_{n-q}^2(\Gamma)J_{m-l}^2(\Gamma) - \sum_n\sum_m\sum_q g_n\beta_{nm}a_q^4J_{m-q}^2(\Gamma)J_{n-q}^2(\Gamma)]. \quad (72)$$

We may alternately write this as

$$\mathcal{P} = \sum_q \alpha_q a_q^2, \quad (73)$$

where, by comparison with (72), α_q is given by

$$\alpha_q = \frac{c}{2L}[\sum_n(\alpha_n - g_n)J_{n-q}^2(\Gamma) + \sum_n\sum_m\sum_l g_n\beta_{nm}a_l^2J_{n-q}(\Gamma)J_{n-l}(\Gamma)J_{m-q}(\Gamma)J_{m-l}(\Gamma) + \sum_n\sum_m\sum_l g_n\beta_{nm}a_l^2J_{n-q}^2(\Gamma)J_{m-l}^2(\Gamma) - \sum_n\sum_m g_n\beta_{nm}a_q^2J_{m-q}^2(\Gamma)J_{n-q}^2(\Gamma)]. \quad (74)$$

The power which is absorbed by all modes may now be equated to the rate of change of total stored energy. From (65) and (73), we then have

$$\sum_q \frac{d}{dt}\left(\frac{a_q^2}{2}\right) + \alpha_q a_q^2 = 0. \quad (75)$$

Since the a_q are normal modes of the lossless system, it is expected that they should independently satisfy (75). From a more physical point of view, we note that the time varying perturbation couples together only the side bands of a particular FM oscillation; thus each oscillation should independently conserve power. We therefore find the set of equations

$$\frac{da_q}{dt} + \alpha_q a_q = 0, \quad (76)$$

where α_q is given by (74), and which at sufficiently large δ should approximately describe the steady state competition among the FM oscillations. We will refer to (76) as the a Equations.

In effect, α_q is the gain constant of the qth oscillation. In a steady state condition such that only the zeroth oscillation is above threshold, its oscillation level may be determined from the condition $\alpha_0 = 0$. In the more general situation, more than one oscillation is above threshold, and the effective gain of any oscillation is dependent on the amplitude of all other oscillations. We note that the a Equations are not expected to correctly describe the transient condition, and instead should be looked at as a stability test for the steady state solutions of the q simultaneous equations $\alpha_q a_q = 0$. Equation (74) indicates a very close coupling of the FM oscillations. In typical situations, a number of FM oscillations may exist at small Γ. However, as Γ is increased, a point is reached above which the strongest of these oscillations

is able to quench all others and establish the desired steady state.

For the special case of completely inhomogeneous saturation, such that the gain of the nth mode is $-g_n(1 - \beta E_n^2)$, i.e., when $\beta_{nm} = \delta_{nm}\beta$, α_q becomes

$$\alpha_q = \frac{c}{2L}\Big[\sum_n (\alpha_n - g_n)J_{n-q}^2(\Gamma) + 2\beta \sum_n \sum_l g_n a_l^2 J_{n-q}^2(\Gamma)J_{n-l}^2(\Gamma) - \beta \sum_n g_n a_q^2 J_{n-q}^4(\Gamma)\Big]. \quad (77)$$

It is of interest to note that in an attempt to determine α_q for the inhomogeneous case of (77) by inspection we probably would have written

$$\alpha_q = \frac{c}{2L} \sum_n [(\alpha_n - g_n) + g_n\beta E_n^2]J_{n-q}^2(\Gamma) \quad \text{(incorrect)}, \quad (78)$$

where, neglecting terms which are phase dependent,

$$E_n^2 = \sum_l a_l^2 J_{n-l}^2(\Gamma). \quad (79)$$

Though the α_q of (78) is very much like that of (77), it differs by a factor of two in describing the saturation of one FM oscillation by another. For the correct α_q of (77), the statement might be made that any FM oscillation saturates another oscillation twice as hard as it saturates itself. This perhaps unexpected factor of two arises due to the power dissipation in the beats of the competing oscillations. It has also been found in simpler problems, such as that of two resonant circuits which are coupled through a nonlinear negative resistance [13].

IX. Variable Modulation Frequency at Constant δ

In previous sections of the paper, we have primarily developed the theory for what may be termed the FM region of operation of an FM laser. However, if either δ or $\Delta\nu$ is sufficiently decreased, the behavior predicted by (13a) and (13b) becomes considerably more complex. In particular, for small detuning, there is a region where the modes have nearly equal amplitudes and is such that the behavior in the time domain consists of a series of spikes or pulses. This type of solution was indicated by (27) of the linear approximation of Section IV, and has been termed as a phase locked solution.

In the numerical analyses of this and the following sections, we assume a Doppler broadened Gaussian atomic line with a homogeneous or natural linewidth which is very small compared with both the axial mode interval and the half-power Doppler width. We include the effects of power independent, but not power dependent mode pulling. Following the notation of Section III, we take

$$g_n = g_0 \frac{Z_i\left(\frac{\nu_n - \omega}{Ku}\right)}{Z_i(0)} \quad (80a)$$

and

$$\sigma_n = g_0 \frac{Z_r\left(\frac{\nu_n - \omega}{Ku}\right)}{Z_i(0)}, \quad (80b)$$

where g_0 is the unsaturated gain at line center, and Z_r and Z_i are the real and imaginary parts of the plasma dispersion function and are described by Lamb [4]. In the limit of vanishingly small homogeneous linewidth, the functions of (80a) and (80b) are the normalized Gaussian and Hilbert transform of the Gaussian, respectively. In these expressions ω is the frequency of the atomic line center and the parameter Ku is a measure of the Doppler broacening; Ku has units of angular frequency and equals 0.6 times the 3 dB Doppler linewidth. It will be convenient to specify the axial mode interval in units of Ku, and thus make use of the tables of Fried and Conte [14]. For the numerical analyses of this section, we take $g_0 = 0.075$, $\alpha_n = 0.070$, and assume an axial mode interval of 0.1 Ku, corresponding to a ratio of Doppler width to mode spacing of 16.67. These conditions correspond to five free-running laser modes above threshold. This situation is somewhat similar to that of some of the experimental work of Ammann, McMurtry, and Oshman [15], and the results of this section may be compared with their work. Mode amplitudes, phases, and frequencies were obtained by digital computer solution of (13a) and (13b). Solution was accomplished by means of a fourth-order Runge–Kutta method. The equations were programed for twenty-one modes ($n = -10$ to $n = +10$) and were run until a steady state solution to three decimal places was reached. Unless otherwise noted in the following, the $n = 0$ mode was taken at line center and thus has a frequency $\nu_0 = \Omega_0 = \omega$.

In Fig. 3, we show laser mode intensities ($\frac{1}{2}E_n^2$) vs. optical frequency—such as would be observed on a scanning Fabry–Perot interferometer. Figure 3(a) shows the intensities of the modes of the free-running laser, i.e., with $\delta = 0$. In Fig. 3(b), δ is set equal to 0.015, and the frequency of the parametric drive is adjusted such that it is exactly equal to the axial mode interval ($\Delta\nu = 0$). A widening of the optical spectrum and some tendency toward equalization of the mode intensities is observed. Relative phases are found to have values between zero and fifty degrees. Of most interest, a uniform, angular frequency shift of all modes from their free-running positions of $\dot{\varphi} = 0.94\ \delta\ \Delta\Omega/\pi$ is obtained. The direction of this shift is dependent on initial conditions, and is too small to show on the scale of Fig. 3. This solution corresponds to that of the phase locked solution of (27) of the linear approximation of Section IV.

In Figs. 3(c) through 3(f), δ is left constant at 0.015, and the detuning $\Delta\nu$ is increased in steps. At the small detuning of Fig. 3(c) ($\Delta\nu = 0.00035\ \Delta\Omega$), we observe an interesting shift of the envelope of the modes of about $2\ \Delta\Omega$. In addition, there is a uniform angular frequency

shift of $\dot{\varphi} = 0.91\ \delta\ \Delta\Omega/\pi$ such as that discussed in connection with Fig. 3(b). Associated with the gross envelope shift is a decrease in laser power as peak relative amplitudes are moved further from the center of the Doppler line. As the detuning is further increased, the envelope shift and decrease in laser power continues, until, as shown in Fig. 3(d), the laser is extinguished.

Figure 3(d) might be considered the beginning of the steady state FM region wherein there is a single FM oscillation with its center frequency at the center of the atomic line, and with a modulation depth Γ which is approximately given by (23). For the detuning of Fig. 3(d), Γ is approximately six, with the result that (55) is not satisfied, and the oscillation is below threshold. In Figs. 3(e) and 3(f), the detuning is further increased, with the result that Γ decreases, relative amplitudes are concentrated closer to the center of the atomic line, and output power increases. In the steady state FM region there is no uniform frequency shift, i.e., $\dot{\varphi}_n = 0$ for all modes. If the detuning is increased past that of Fig. 3(f), we enter the region of multiple FM oscillation that was considered in Section VIII. In this region more than one mode may act as a carrier for an FM oscillation, and a steady state solution in the sense of zero $\dot{E}_n$ does not exist.

Figure 4 shows the time domain behavior which corresponds to the spectrum of Figs. 3(b) and 3(f). If the output signal of the laser is written

$$E(t) = \sum_n E_n \cos\left[(\Omega_0 + n\nu_m)t + \varphi_n\right], \tag{81}$$

then the low passed portion (or envelope) of $E^2(t)$, such as would be obtained if the signal were incident on a photodetector, is given by

$$W(t) = \tfrac{1}{2} \sum_s \sum_n E_n E_{n+s} \cos\left(s\nu_m t + \varphi_{n+s} - \varphi_n\right). \tag{82}$$

The data for Fig. 4 were obtained by evaluation of (82) for the E_n and φ_n, corresponding to Figs. 3(b) and 3(f). Output intensities are normalized to the total average intensity ($\frac{1}{2}\sum_n E_n^2$) of the free-running laser. We note that the pulsing of the phase locked solution is at the driving frequency of the internal phase perturbation and has peak intensities which are approximately six times the average intensity of the free-running laser. By contrast, the envelope which corresponds to the FM spectrum of Fig. 3(f) is more nearly constant and independent of time. The ripple is entirely even harmonic, and is a result of the distortion of amplitudes and phases from those of an ideal FM signal. As will be seen in the following section, this ripple can be made arbitrarily small, if δ is made sufficiently large. As opposed to the periodic behavior of both the phase locked and FM solutions, we note that the time domain behavior of the envelope of a free-running laser consists of an erratic fluctuation, with peak intensities almost as great as those obtained in the phase locked region.

In Fig. 5 we show output power ($\frac{1}{2}\sum_n E_n^2$) as a function of the normalized detuning. Output power is normalized

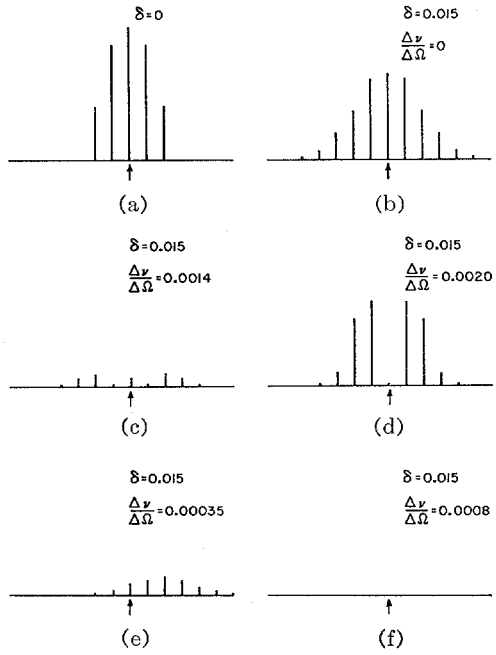

Fig. 3. Laser mode intensities at constant δ and variable detuning: $g_0 = 0.075$; $\alpha_n = 0.070$; $\Delta\Omega = 0.1$ Ku. (Five modes free running.)

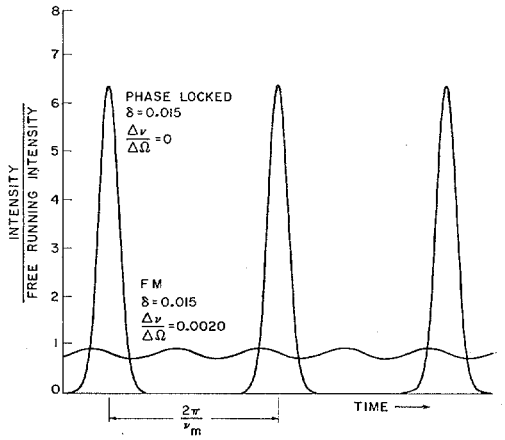

Fig. 4. Output intensity vs. time for phase-locked and FM operation: $g_0 = 0.075$; $\alpha_n = 0.070$; $\Delta\Omega = 0.1$ Ku. (Five modes free running.)

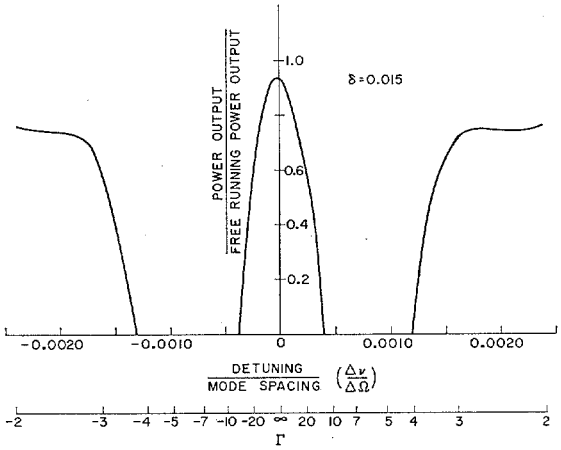

Fig. 5. Output power vs. detuning: $g_0 = 0.075$; $\alpha_n = 0.070$; $\Delta\Omega = 0.1$ Ku. (Five modes free running.)

to that of the free-running laser, and the conditions are again those of Figs. 3 and 4. At zero detuning, output power is about 0.95 that of the free-running laser. As detuning is increased, the mode envelope shifts away from the center of the Doppler line and output power decreases to zero. The oscillation remains below threshold until a detuning corresponding to a Γ of ~ 4. For a further increase of detuning, Γ decreases and the output power rapidly rises. We note that for the case considered, either phase-locked or FM operation may be obtained at nearly full power of the free-running laser.

In Figs. 3 and 4 we considered only positive detunings; that is, we assumed the modulation frequency to be less than the axial mode interval. For negative detunings we obtain very similar results, the one difference being a small asymmetry in frequency. This asymmetry is seen in the power curve of Fig. 5, and was first observed in the experiments of Ammann, McMurtry, and Oshman.[7] It is seen from Fig. 5 that the asymmetry appears in both the phase-locked and FM regions. Peak power in the phase-locked region occurs at a detuning of $\Delta\nu = -0.0004\ \Delta\Omega$ rather than zero. For positive detuning, threshold for the FM region occurs at $0.0012\ \Delta\Omega$, while for negative detuning it occurs at $-0.0013\ \Delta\Omega$. It is found that Γ's obtained with a positive detuning are slightly smaller than those predicted by (23), while Γ's obtained with a negative detuning are slightly larger than those of (23).

These asymmetries may be explained in terms of nonlinear but power independent mode pulling. That is, they are a result of the portion of the plasma dispersion function Z_r which depends nonlinearly upon frequency. Qualitatively, we note that, for an inverted atomic media, the effect of the nonlinear terms in the series expansion of Z_r is to decrease the index of refraction of modes above the center of the atomic line and to increase the index of refraction of modes below the center of the atomic line. These terms thus act to push all modes further from the center of the atomic line than they would otherwise be. The result is that, for negative detuning (modulation frequency greater than the axial mode interval), the average separation between the modulation sidebands and axial modes is somewhat smaller than it would otherwise be; thus, some sort of averaged detuning is somewhat smaller than that which would be obtained in the absence of this nonlinear part of χ_n'. For positive detuning, the opposite situation holds, and an averaged detuning is somewhat larger than that obtained in the absence of mode pulling. This asymmetrical behavior is a distortion and, as predicted by the form of μ_n of (53), will become increasingly small if, at constant Γ, δ becomes increasingly large. From an alternate point of view, if the same Γ is obtained at an increased δ, then $\Delta\nu$ must be increased, and the nonlinear mode pulling is more effectively swamped out.

The behavior in the phase locked region is at first somewhat puzzling; that is, it is physically hard to see how pulsing should result from a time varying phase perturbation. A qualitative explanation is indicated by Fig. 6, which is a plot of $\dot{\varphi}/\Delta\nu$ vs. Γ (or equivalently $\Delta\nu$) at constant δ. Since $\dot{\varphi}$ is a uniform shift of all modes from their assumed positions of (10), the closest integer to $\dot{\varphi}/\Delta\nu$ indicates that mode which is closest to an unperturbed cavity resonance. The curve in Fig. 6 begins at Γ large enough such that the single FM oscillation having its center frequency at the center of the atomic line is already below threshold. As detuning is decreased and thus Γ is increased, a point is reached such that an oscillation with its carrier, i.e., its on-resonance frequency component, at approximately the $+12$ mode, comes above threshold. However, at the given δ the distortion of this oscillation is so large that it bears no resemblance to an FM signal. As $\Delta\nu$ is further decreased, we find that $\dot{\varphi}$ is approximately $\delta\Delta\Omega/\pi$ [the value predicted by (27)], and thus $\dot{\varphi}/\Delta\nu \sim \Gamma$. For large Γ, $J_n(\Gamma)$ has its peak amplitude at approximately $n = \Gamma$. It thus appears that what is happening is that the oscillation which, if undistorted, would have its peak relative amplitude at approximately the center of the atomic line is the one which oscillates—though with a distortion which eliminates most of the FM spectrum.

The foregoing explanation of the phase-locked region leads to the prediction that if δ were increased to the point where the signal were better able to maintain its outer sidebands, its power should decrease; and at a sufficiently large δ, it should fall below threshold. This is indeed the case as is shown in Fig. 7. Here δ is increased over Figs. 3 through 6 by a factor of five, and normalized power vs. normalized detuning is again plotted. We find that the phase-locked solution is completely eliminated. We also note that, due to the larger δ, the asymmetry of Fig. 5 is significantly reduced.

The behavior vs. detuning that has been seen in Figs. 3 through 7 has been somewhat simpler than it would have been had δ not been chosen sufficiently large. At low δ, the region over which the laser is extinguished becomes an unquenched region wherein $\dot{E}_n \neq 0$ and a number of highly distorted FM oscillations are above threshold. (Alternately, this region might be considered as one consisting of multiple phase-locked solutions.) At still lower δ this unquenched region extends into what was previously the steady state FM region. Finally, for very low δ, i.e., δ considerably smaller than the excess gain,[8] the FM solution entirely disappears. There remains a steady state phase-locked solution for very small $\Delta\nu$, and for all other $\Delta\nu$ the situation is unquenched. If spontaneous emission is neglected, then as $\Delta\nu$ approaches zero, the δ which is necessary to obtain a phase-locked

[7] In their paper entitled "Detailed Experiments on Helium-Neon FM Lasers," Ammann, McMurtry, and Oshman have defined their detuning oppositely from that of this paper. That is, their detuning is positive when the modulation frequency is greater than the axial mode interval. Allowing for this difference in definition, the direction of our asymmetry is still opposite to theirs. This is perhaps due to a difference in definition of $\Delta\Omega$.

[8] We define the excess gain as the difference between the unsaturated single pass gain at line center and the single pass loss.

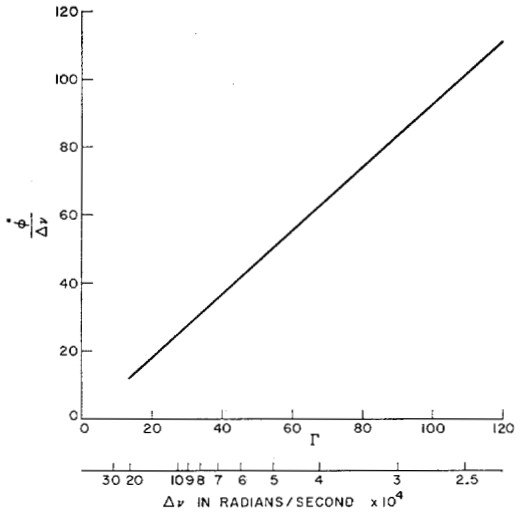

Fig. 6. $\dot{\varphi}/\Delta\nu$ vs. Γ: $g_0 = 0.075$; $\alpha_n = 0.070$; $\Delta\Omega = 0.1$ Ku (Five modes free running.)

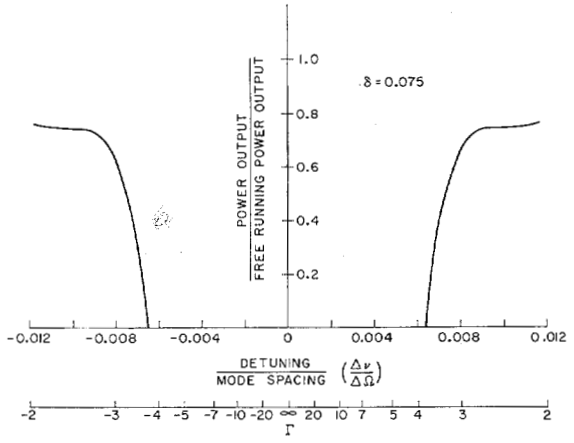

Fig. 7. Output power vs. detuning for larger δ: $g_0 = 0.075$; $\alpha_n = 0.070$; $\Delta\Omega = 0.1$ Ku. (Five modes free running.)

solution also approaches zero. In such small δ cases, the final steady state mode amplitudes are approximately those of the free-running laser, and the principal effect of the perturbation is to cause a locking of the phases of the respective modes. The effect on the phase-locked solution of increasing δ is to cause the mode amplitudes to become more nearly equal and to extend over a larger spectral width than did the modes of the free-running laser. The result is a sharpening of the time domain pulsing and a decrease in output power. The time domain pulses may be made increasingly sharp until the laser is extinguished.

X. Distortion and Super-Mode Conversion

In this section we apply the iterative procedure of Sections V through VII and study some effects of distortion of the ideal FM solution. We assume a somewhat higher gain than in the previous section and take $g_0 = 0.085$, and $\alpha_n = 0.070$. Inhomogeneous saturation, i.e., $\beta_{nm} = \beta\delta_{nm}$ and a ratio of Doppler width to mode spacing of 16.67 are again assumed. These conditions correspond to nine free-running modes in the unperturbed laser.

In Tables I and II we consider mode amplitudes and mode phases, respectively, for a case where $\delta = 0.06$, and the detuning is such that $\Gamma = 4.5$.[9] Column 1 of Table I shows the ideal Bessel function amplitudes which would exist if all net saturated gains were zero and mode pulling were neglected. Column 2 gives the results of digital computer solution of (13a) and (13b). Columns 3, 4, and 5 give the results of the first, second, and third iterations of the procedure of Section VII. In Table II, similar results are given for the relative phase angles. It is noted that these phase angles differ considerably more from their ideal values than do the amplitudes of Table I.

In cases where the distortion is larger than that of the previous example, for instance when δ is considerably lower or Γ is considerably larger, the convergence rate of the iterative procedure will be slower. If the constants of this example are left unchanged, except for reducing both δ and $\Delta\nu$ by a factor of two, it is found that about five iterations are required to reach a comparable steady state. However, even at five iterations, the iterative procedure requires only about 1/20 of the computer time as does solution of (13a) and (13b) to comparable accuracy. During the course of the numerical work, a few cases were found where the numerical procedure failed to converge. These were cases of high distortion and occurred particularly at large Γ.

One manifestation of distortion is the existence of beats when the output of an FM laser is incident on a photodetector. Proceeding from (82) it is seen that the amplitude R_q and phase η_q of the qth beat between the laser modes is given by

$$R_q = (M_q^2 + N_q^2)^{1/2}$$
$$\eta_q = \tan^{-1}\left(\frac{N_q}{M_q}\right), \tag{83}$$

where

$$M_q = \tfrac{1}{2}\sum_n E_n E_{n+q}\cos(\varphi_{n+q} - \varphi_n)$$
$$N_q = \tfrac{1}{2}\sum_n E_n E_{n+q}\sin(\varphi_{n+q} - \varphi_n). \tag{84}$$

For the ideal situation where $E_n = J_n(\Gamma)$ and $\varphi_n - \varphi_{n-1} = 0$, by noting (39) we see that all beats for $q \neq 0$ are zero.

Even in the actual case wherein net saturated gains and mode pulling are not zero, it may be shown from the

[9] The presence of a linear term in χ'_n in effect changes the axial mode interval and complicates the specification of the detuning which will lead to a given Γ. The function Z_r of (80b) may be expanded in a power series as follows [14]:

$$Z_r(\zeta) = +2\zeta\left[1 - \frac{2\zeta^2}{3} + \frac{4\zeta^4}{15} - \frac{8\zeta^6}{105} + \cdots\right].$$

If accounted for as part of the detining, the linear term of this series does not lead to distortion. We will thus adopt the procedure of neglecting this term in Ψ_n of (28a), and instead will include its effect in the specification of the detuning. We note that experimentally this problem does not arise in that the linear portion of the mode pulling is automatically included in the measurement of the axial mode interval.

TABLE I

COMPARISON OF MODE AMPLITUDES (E_n)

$g_0 = 0.085$

$\alpha_n = 0.070$

$\left[\frac{\text{Doppler Width}}{\text{Mode Spacing}}\right] = 16.67$

9 Modes Free Running

$\delta = 0.06$

$\Gamma = 4.5$

n	Ideal (Bessel Functions)	Equations (13a) and (13b)	Iterative Procedure		
			1st Iteration	2nd Iteration	3rd Iteration
0	−0.320	−0.279	−0.282	−0.280	−0.280
1	−0.231	−0.251	−0.254	−0.252	−0.252
2	0.218	0.180	0.180	0.180	0.180
3	0.425	0.410	0.413	0.412	0.412
4	0.348	0.367	0.368	0.369	0.369
5	0.195	0.223	0.222	0.224	0.225
6	0.084	0.107	0.104	0.107	0.107
7	0.030	0.043	0.043	0.042	0.043
8	0.009	0.015	0.014	0.014	0.015
9	0.002	0.005	0.004	0.004	0.005
10	0.001	0.001	0.001	0.001	0.001

TABLE II

COMPARISON OF PHASE ANGLES ($\varphi_n - \varphi_{n-1}$)

$g_0 = 0.085$

$\alpha_n = 0.070$

$\left[\frac{\text{Doppler Width}}{\text{Mode Spacing}}\right] = 16.67$

9 Modes Free Running

$\delta = 0.06$

$\Gamma = 4.5$

n	Ideal	Equations (13a) and (13b)	Iterative Procedure		
			1st Iteration	2nd Iteration	3rd Iteration
1	0°	5.223°	5.183°	5.194°	5.242°
2	0°	−22.181°	−18.583°	−21.178°	−22.158°
3	0°	17.611°	14.311°	17.645°	17.622°
4	0°	6.298°	4.899°	6.219°	6.352°
5	0°	4.763°	3.730°	4.590°	4.746°
6	0°	5.841°	4.909°	5.611°	5.796°
7	0°	7.317°	6.254°	7.008°	7.265°
8	0°	8.598°	7.290°	8.139°	8.496°
9	0°	9.395°	8.020°	8.919°	9.363°
10	0°	8.977°	8.480°	8.951°	9.310°

formulas of Section VII that, if the center frequency of the FM oscillation is at the center of a symmetrical atomic line, then all odd harmonic beats will be identically zero.

Figure 8 shows the amplitude of the second beat vs. δ at constant Γ. That is, both δ and $\Delta\nu$ are varied such that Γ as given by (23) remains constant. Beat amplitudes are normalized to the total intensity of the FM laser at the given Γ. For reference, the beat which is obtained from (83) by taking the E_n as those of the free-running laser, and assuming that relative phases are zero, is noted in Fig. 8. These conditions are comparable to what has been termed a selflocked beat and which is often observed in practice [10], [15]. Beat amplitudes are shown for $\Gamma = 4.5$ and for $\Gamma = 3.0$. We note that distortion is somewhat larger at the larger Γ, and for either Γ, decreases as δ is increased.

Figure 9 shows the time domain behavior corresponding to certain of the points of Fig. 8. Data for this figure were obtained by evaluation of (82) using E_n and φ_n obtained by five iterations of the procedure of Section VII. It is seen that the ripple may be made increasingly small if δ is made sufficiently large.

As another figure of merit for an FM signal, we consider its supermode conversion efficiency. The super-mode technique is shown schematically in Fig. 10, and was suggested by Massey and demonstrated by Massey, Oshman, and Targ [16]. In this technique the output signal from an FM laser is passed through an external phase modulator which is driven such that its single pass phase retardation is exactly equal to the Γ at which the FM laser is running. By properly adjusting the phase of the external modulator with respect to that of the internal phase perturbation, the resultant light signal can be made to have a modulation depth anywhere between zero and 2Γ. In particular, when the resultant modulation depth is adjusted to zero, then in principal, all of the energy that was previously distributed between all of the sidebands of the FM signal should appear as a single monochromatic optical signal—or "super-mode," as it has been termed by Targ.

We take the light signal emerging from the FM laser to be of the form of (81), and assume the single pass phase retardation of the external modulator to be $-\Gamma \sin \nu_m t$. Each sideband of the FM signal is thus modulated, and after passage through the external modulator, we have

$$E_0(t) = \sum_n E_n \cos [(\Omega_0 + n\nu_m)t + \varphi_n - \Gamma \sin \nu_m t]. \quad (85)$$

By using various trigonometric and Bessel identities it may be shown that $E_0(t)$ may be written

$$E_0(t) = \sum_q F_q \cos (\Omega_0 + q\nu_m)t + \sum_q H_q \sin (\Omega_0 + q\nu_m)t, \quad (86)$$

where F_q and H_q are given by

$$F_q = \sum_n E_{q+n} J_n(\Gamma) \cos \varphi_{q+n}$$
$$H_q = -\sum_n E_{q+n} J_n(\Gamma) \sin \varphi_{q+n}. \quad (87)$$

The power in the desired super-mode is then $F_0^2 + H_0^2$. We define the super-mode conversion efficiency to be the ratio of power in the super-mode to the total power of the incident FM signal, giving

$$\text{super-mode conversion efficiency} = \frac{(F_0^2 + H_0^2)}{\sum_q (F_q^2 + H_q^2)}. \quad (88)$$

Figure 11 shows super-mode conversion efficiency vs. δ at constant Γ for the case of nine free-running modes.

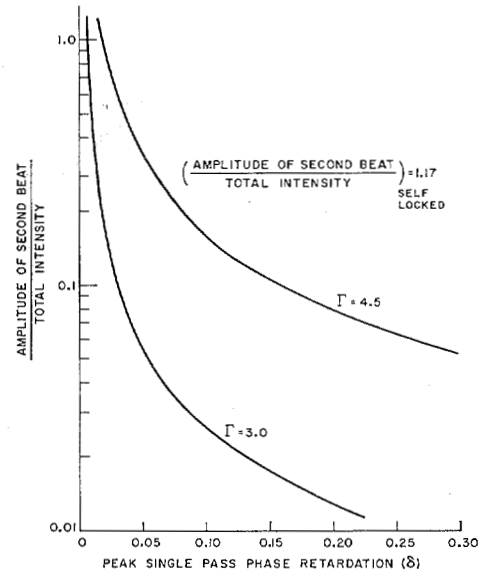

Fig. 8. Amplitude of second beat vs. δ: $g_0 = 0.085$; $\alpha_n = 0.070$; $\Delta\Omega = 0.1$ Ku. (Nine modes free running.)

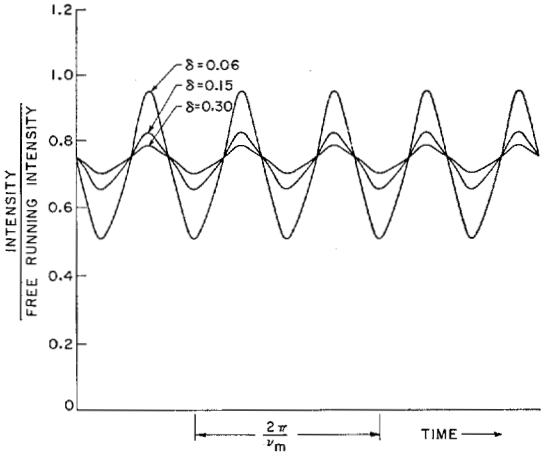

Fig. 9. Output intensity vs. time at different δ: $g_0 = 0.085$; $\alpha_n = 0.070$; $\Delta\Omega = 0.1$ Ku. (Nine modes free running.)

At a $\Gamma = 3.0$, a δ approximately equal to five times the excess gain yields a conversion efficiency of almost 100 percent. At $\Gamma = 4.5$, a somewhat larger δ is required. In obtaining these conversion efficiencies from (88) we have used the Γ as given by (23) and have properly taken into account the linear part of χ_n'. It has been previously noted, however, that because of the nonlinearity of mode pulling vs. frequency, this Γ is not the closest approximation to the existing FM signal. It is thus likely that the efficiencies of Fig. 11 could be somewhat increased by a more optimum choice of the converting Γ.

Examination of the time domain behavior of the converted signal shows that the super-mode process leaves the AM ripple unchanged. At $\delta = .06$, Fig. 9 shows the FM signal to have about a 30 percent AM ripple, while Fig. 11 shows the super-mode conversion efficiency to be about 98 percent. Though at first surprising, the converted signal is found to have a time domain behavior which is identical to that of Fig. 9.

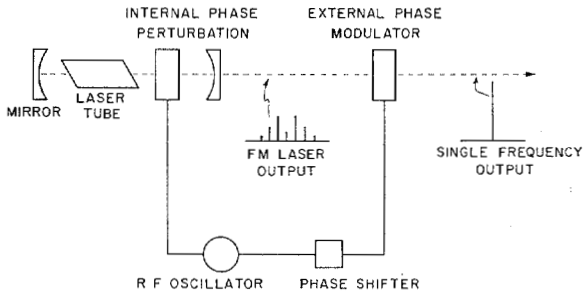

Fig. 10. Schematic of super-mode technique.

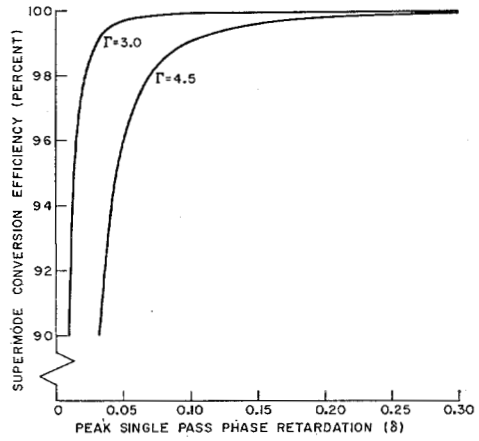

Fig. 11. Super-mode conversion efficiency vs. δ: $g_0 = 0.085$; $\alpha_n = 0.070$; $\Delta\Omega = 0.1$ Ku. (Nine modes free running.)

XI. Application and Validity of the a Equations

In the derivation of the a Equations of Section VIII, two approximations were made. First, it was assumed that δ was sufficiently large that the competing oscillations could be considered to have exactly Bessel function amplitudes. Second, and more important, it was assumed, or perhaps hoped, that phase-locking between different FM oscillations could be neglected without affecting the range of Γ over which only a single steady state FM oscillation would exist. Unfortunately, in certain cases, this second assumption does not appear to be valid.

The thin curve of Fig. 12 shows the application of the a Equations to the case of nine free-running modes of the previous section. Inhomogeneous saturation of all modes is again assumed, and amplitudes of all oscillations are normalized to the total power of the free-running laser. When $\Gamma = 0$, the FM oscillations are identical to the free-running modes. As Γ is slightly increased, the oscillations remain very weakly coupled, and all nine FM oscillations exist simultaneously. For a somewhat larger Γ, certain of these oscillations are quenched, but a condition of multiple oscillation persists. When $\Gamma = 2.3$ or larger, quenching is complete and only the zeroth oscillation remains. Output power first rises as a result of more effective atomic saturation. The slight dip at $\Gamma \sim 3.8$ is attributable to a decrease in amplitude of the one mode, i.e., $J_1(3.832) = 0$. For larger Γ power decreases as relative amplitudes which are further from the center of the Doppler line are increased; and for $\Gamma = 6.7$ the oscillation is below threshold.

The thick curve in Fig. 12 shows normalized output power as obtained from (13a) and (13b), where a δ of 0.06 has been assumed. In regions where this thick line is absent, (13a) and (13b) predict a condition of multiple FM oscillation. Thus, at points where there is only a single thin line and no thick line, (13a) and (13b) are in disagreement with the a Equations.[10]

At Γ's where the a Equations predict multiple FM oscillations, (13a) and (13b) are in agreement. For certain of these cases, the time variation of the nonsteady state E_n which resulted from the digital computer solution of (13a) and (13b) were examined. At $\Gamma = 2.15$, where the a Equations predict that the a_0 and the $a_{\pm 1}$ oscillations should exist simultaneously, that all the E_n were periodic functions of time and had a fundamental frequency variation of $\Delta\nu$ and a higher harmonic variation of $2\Delta\nu$. At $\Gamma = 1.35$, where the a Equations predict that only the $a_{\pm 2}$ oscillations should exist, all the E_n had a perfectly sinusoidal time variation at a frequency of $4\Delta\nu$. These results are consistent with the transformation of (61).

Examination of the time domain behavior of the E_n at $\Gamma = 2.5$, i.e., one of the points of disagreement, showed the zero and also the ± 1 oscillations to exist simultaneously. It was also determined that irrespective of initial conditions, these oscillations existed with a phase relation which, if each were perfect FM, results in partial cancellation of the factor of two which is involved in the cross saturation of FM oscillations, and which was discussed at the end of Section VIII.

It thus appears that the a Equations are over optimistic, and predict a steady state FM oscillation, when perhaps a phase-locked multiple oscillation situation would exist. We note, however, that we have assumed a perfectly symmetrical atomic line with one FM oscillation exactly at its center. This condition is favorable to a phase-locking process, and whether such locking will occur under typical experimental conditions remains to be determined.[11]

As another application of the a Equations, we considered the case of a very narrow high gain line such that only one free-running mode was above threshold. An axial mode interval equal to 1.2 times the Doppler width was assumed, and g_0 and α were taken as 0.56 and 0.056, respectively. The results are shown in Fig. 13, where two interesting effects are observed. First, we find that

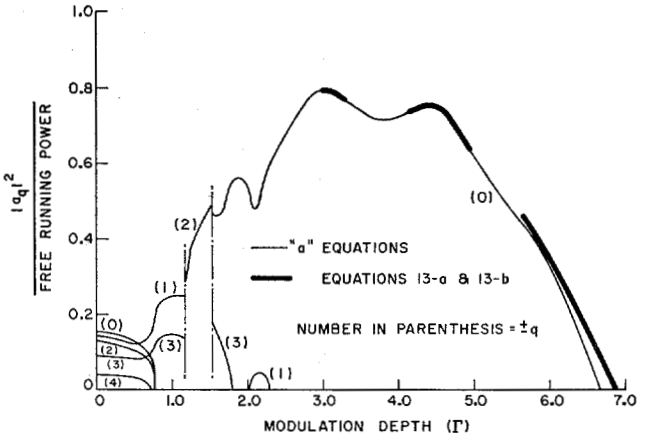

Fig. 12. $|a_q|^2$ vs. Γ: $g_0 = 0.085$; $\alpha_n = 0.070$; $\Delta\Omega = 0.1$ Ku. (Nine modes free running.)

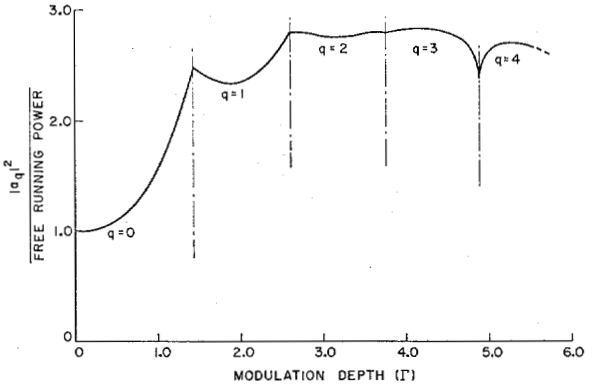

Fig. 13. $|a_q|^2$ vs. Γ for high gain line: $g_0 = 0.56$; $\alpha_n = 0.056$; $\Delta\Omega = 2.0$ Ku. (One mode free running.)

the FM power may exceed that of the free-running laser by a factor of ~ 3. Second, we find that, for higher Γ, steady state FM oscillations which have their carrier frequency either above or below the center of the atomic line may exist. In such cases, whether the plus or minus oscillation exists is determined by initial conditions.

For the case of the high gain line, as well as another case which was considered wherein only two FM oscillations were above threshold, it was found that the results of the a Equations were in complete agreement with those of (13a) and (13b). The agreement in these cases is attributed to the fact that a phase-locking of oscillations requires at least three oscillations—two of which drive the third. It is planned that a further study of phase-locking of FM oscillations will be undertaken.

XII. Effect of Mirror Motion

In previous sections we have always assumed that the center frequency of the $q = 0$ oscillation was at the center of a symmetrical atomic line. Under typical operating conditions, this will seldom be the case. As a result of mirror motion, the center frequencies of all the FM oscillations will drift with respect to the center of the atomic line. It is expected that if the drift from the center of the atomic line is greater than about one-half an axial mode interval, then either the $q = -1$ or $q = +1$ oscillation should become the dominant oscillation. This

[10] Since in all cases the modes display a transient which generally takes the form of a damped or growing beat at harmonics of $\Delta\nu$, it is necessary to make an arbitrary decision as to what is to be considered as a steady state condition. For the present case, a 10 percent variation of the E_n after 100 microseconds was considered as satisfactory. At a proper iteration interval this represents a run time of between 15 and 30 minutes on an IBM 7090, for each data point.

[11] In their experiments on a 6328A He-Ne laser with nine free-running modes above threshold, Ammann, McMurtry, and Oshman, [15], have found that a steady state FM oscillation does exist at certain points, e.g., $\Gamma = 3.9$, where for a running time of 100 μs, (13a) and (13b) predict multiple oscillation. However, this does not resolve the question, in that completely inhomogeneous saturation is not a proper approximation for He-Ne. We have found that if a single pass gain of the form $g_n(1 - \beta E_n^2 - 0.4\,\beta E_{n+1}^2 - 0.4\,\beta E_{n-1}^2)$ is assumed, and all other constants are left unchanged, that (13a) and (13b) will then also predict a steady state oscillation at $\Gamma = 3.9$.

type of jumping behavior has been observed by Ammann, McMurtry, and Oshman [15]. From the point of view of the super-mode conversion process, the resultant super-mode will be stable to within about $\pm\frac{1}{2}$ of an axial mode interval from the center of the atomic line.

In Section X it was noted that if the center frequency of an FM oscillation is at the center of a symmetrical atomic line, then all odd harmonic beats will be identically zero. This results because the contributions to the odd harmonic beats from sidebands which are above the center frequency of the FM oscillation are exactly cancelled by contributions from sidebands below the center frequency of the oscillation. As the center frequency moves off line center, this will no longer be the case. The cancellation of upper and lower contributions is no longer complete, and odd harmonic distortion rapidly increases.

Figures 14 and 15 show the amplitude and phase, respectively, of the first and second beats as a function of the position of the center frequency of the FM oscillation with respect to the center of the atomic line. For these figures, $\delta = 0.15$, $\Gamma = 3.0$, and other constants and the normalization are the same as those of Fig. 8. Data for the figures were obtained by five iterations of the procedure of Section VII. It is seen that the amplitude of the first beat is extremely sensitive to the position of the center frequency of the FM oscillation, while the amplitude of the second beat is nearly independent of this position. In addition, the phase of the first beat changes abruptly as the center of the FM oscillation moves from one side of the atomic line to the other. The behavior of higher odd and even beats is similar to that of the first and second beats, respectively. Harris and Oshman have proposed that these effects could be used as a frequency discriminant for stabilization of an FM laser, and experiments demonstrating the existence of such a discriminant have been performed [17].

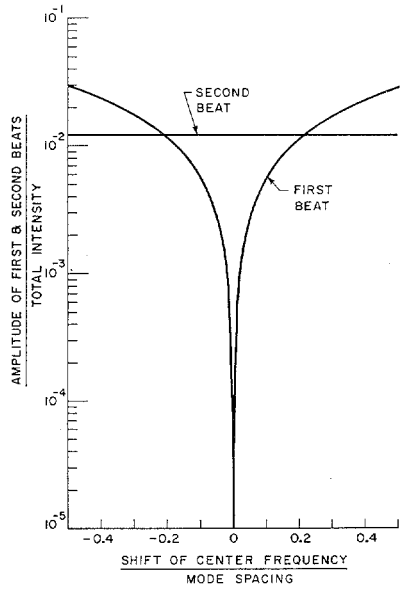

Fig. 14. Amplitude of first and second beat vs. position of center frequency: $g_0 = 0.085$; $\alpha_n = 0.070$; $\Delta\Omega = 0.1$ Ku. (Nine modes free running.)

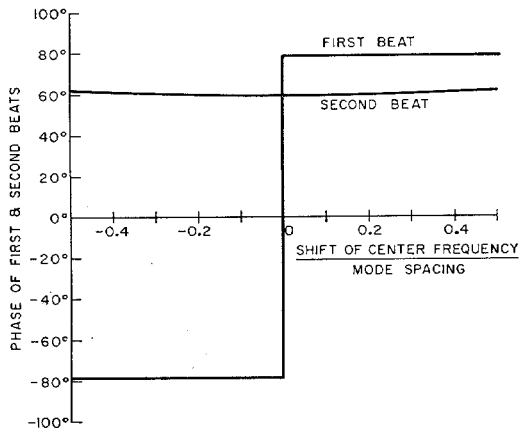

Fig. 15. Phase of first and second beat vs. position of center frequency: $g_0 = 0.085$; $\alpha_n = 0.070$; $\Delta\Omega = 0.1$ Ku. (Nine modes free running.)

Acknowledgment

The authors wish to express their gratitude to E. O. Ammann, B. J. McMurtry, and M. K. Oshman for providing us with the results of their experiments on He-Ne FM lasers, and also for numerous helpful discussions. Knowledge of their experiments increased our confidence in the theory, and in certain instances indicated the direction in which to proceed. We also wish to thank L. Osterink, A. E. Siegman, and Russell Targ for interesting discussions; and gratefully acknowledge the assistance of Mrs. Cora Barry with the numerical computation.

References

[1] W. R. Bennett, Jr., "Hole burning effects in a He-Ne optical maser," *Phys. Rev.*, vol. 126, pp. 580–593, April 1962.
[2] C. L. Tang, H. Statz, and G. de Mars, "Spectral output and spiking behavior of solid-state lasers," *J. Appl. Phys.*, vol. 34, pp. 2289–2295, August 1963.
[3] S. E. Harris and R. Targ, "FM oscillation of the He-Ne laser," *Appl. Phys. Letters*, vol. 5, pp. 202–204, November 1964.
[4] W. E. Lamb, Jr., "Theory of an optical maser," *Phys. Rev.*, vol. 134, pp. A1429–A1450, June 1964.
[5] E. I. Gordon and J. D. Rigden, "The Fabry–Perot electro-optic modulator," *Bell Sys. Tech. J.*, vol. XLII, pp. 155–179, January 1963.
[6] A. Yariv, "Internal modulation in multimode laser oscillators," *J. Appl. Phys.*, vol. 36, pp. 388–391, February 1965.
[7] S. E. Harris and O. P. McDuff, "FM laser oscillation-theory," *Appl. Phys. Letters*, vol. 5, pp. 205–206, November 1964.
[8] L. E. Hargrove, R. L. Fork, and M. A. Pollack, "Locking of He-Ne laser modes induced by synchronous intracavity modulation," *Appl. Phys. Letters*, vol. 5, pp. 4–5, July 1964.
[9] M. DiDomenico, Jr., "Small-signal analysis of internal (coupling type) modulation of lasers," *J. Appl. Phys.*, vol. 35, pp. 2870–2876, October 1964.
[10] M. H. Crowell, "Characteristics of mode-coupled lasers," *IEEE Journal of Quantum Electronics*, vol. QE-1, pp. 12–20, April 1965.
[11] B. Friedman, *Principles and Techniques of Applied Mathematics*. New York: Wiley, 1956.
[12] M. Abramowitz and I. A. Stegun, *Handbook of Mathematical Functions*. National Bureau of Standards, Applied Mathematics Series, vol. 55, 1964, p. 363.
[13] W. J. Cunningham, *Introduction to Nonlinear Analysis*. New York: McGraw-Hill, 1958, p. 313.
[14] B. D. Fried and S. D. Conte, *The Plasma Dispersion Function (Hilbert Transform of the Gaussian)*. New York: Academic, 1961.
[15] E. O. Ammann, B. J. McMurtry, and M. K. Oshman, "Detailed experiments on helium-neon FM lasers," this issue, pp. 263–272.
[16] G. A. Massey, M. K. Oshman, and R. Targ, "Generation of single frequency light using the FM laser," *Appl. Phys. Letters*, vol. 6, pp. 10–11, January 1965.
[17] S. E. Harris, M. K. Oshman, B. J. McMurtry, and E. O. Ammann, "Proposed frequency stabilization of the FM laser," Appl. Phys. Letters, vol. 7, pp. 184–186, October 1965.